UNIVERSITY OF SASKATCHEWAN

SPIN Subatomic Physics Institute
Physics and Engineering Physics
University of Saskatchewan

Photonuclear Reactions at HIGS using Blowfish

Rob Pywell

W. Wurtz, G. Pridham, M. Sharma, O. Mavrichi, R. Igarashi, University of Saskatchewan*; B. Norum, S. Kucuker, S. Tkachenko, R.A. Lindgren, P.-N. Seo, R. Duve,* University of Virginia*, Charlottesville, VA; B. Sawatzky*, Jefferson Laboratory, Newport News, VA; *H. Weller, L. Meyers, S. Stave, M. Blackston,* Duke University, Durham, NC; *M. Ahmed, North* Carolina Central University, Durham, NC; *G. Feldman*, George Washington University; *K. Fissum,* Lund University, Lund, Sweden

Precision Photonuclear Reaction Measurements

- Precision theoretical calculations for light nuclei are now possible.
- In general photonuclear measurements do not have the precision to be helpful in interpreting the results of recent high quality calculations.
- Except for a few recent measurements – photonuclear reaction measurements in the past, have not paid attention to ensuring that systematic uncertainties are properly estimated and kept under control.
- The obvious example is ^4He.

^{4}He Photodisintegration

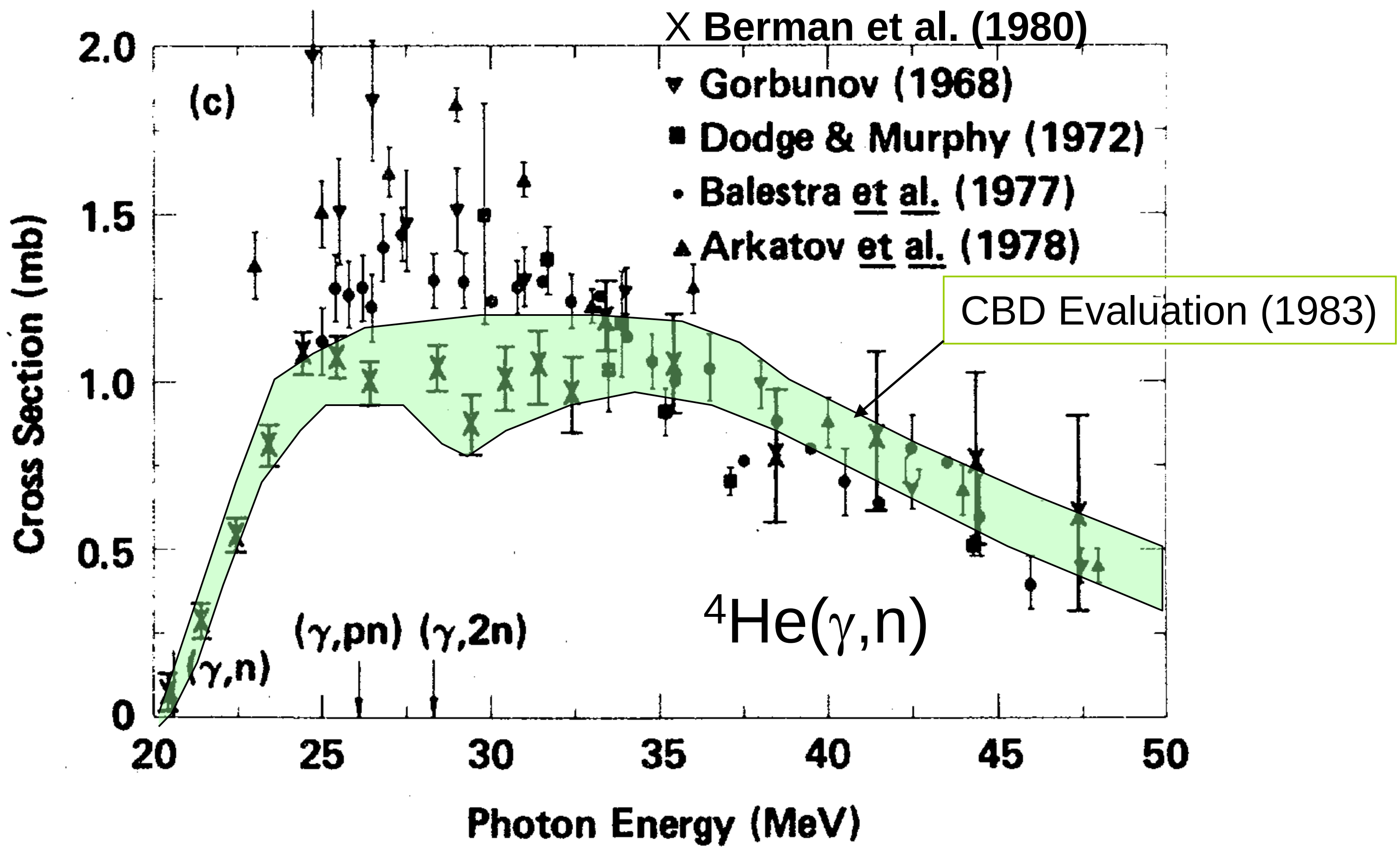

Berman et al. PRC 22 (1980) 2273

^{4}He Photodisintegration

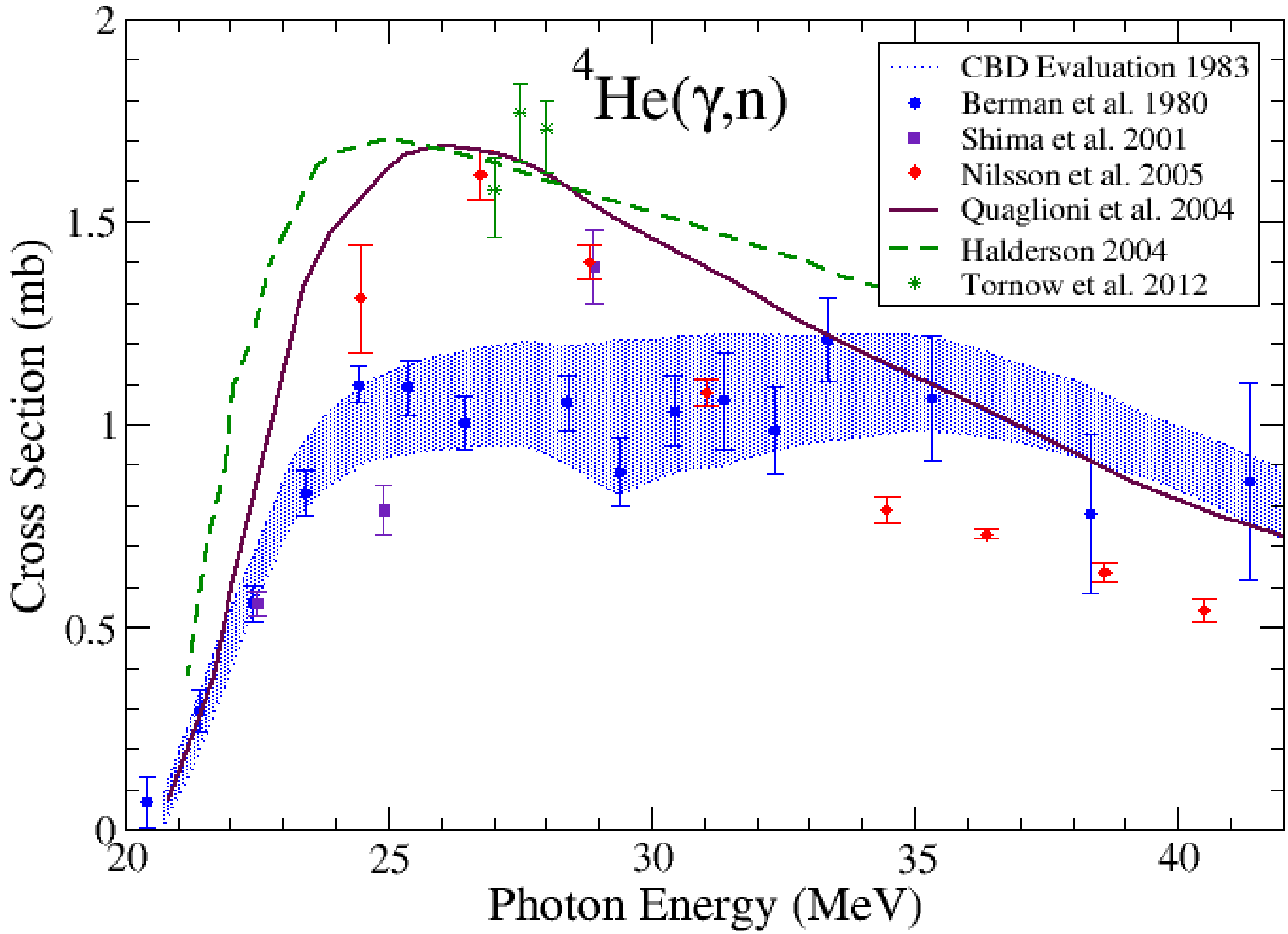

Systematic Uncertainties

- Only the most recent measurement have paid strict attention to systematic uncertainties.
- The most difficult parameters to determine are
  - Detector efficiencies
  - Number of incident photons
- There is no value in making new measurements unless systematic uncertainties are shown to be under control.
- I hope to convince you that measurements with systematic uncertainties less than about 3% are now possible.

Precision Absolute Cross Sections

- In this talk I will concentrate on photoneutron cross sections.
- Specifically – measured at HIγS using the Blowfish neutron detector.
- HIγS has several advantages for these measurements.
  - Monoenergetic photons (low ΔE)
  - High intensity ($> 10^7$ s^{-1})
  - Linear and circular polarization available
  - Pulsed (micropulses every ~180 ns)

Blowfish

- Large solid angle neutron detector
- 88 BC-505 liquid scintillators
  - Spherically arranged on a 16 inch radius.
  - Covers ¼ of 4 π sr.
  - Pulse shape discrimination.

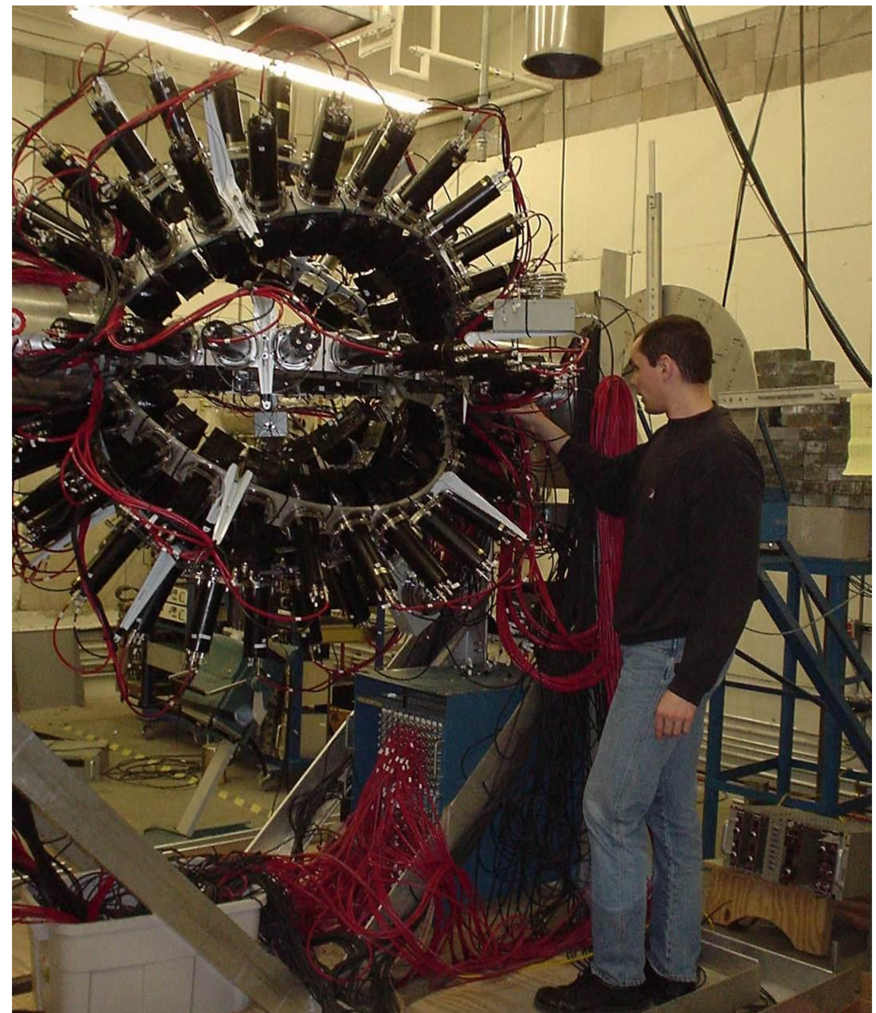

GEANT4 Simulation

- Simulation for Blowfish has been built using the GEANT4 toolkit (C++)
- Vital to the process of determining the detector efficiency.
- Augmented with modules to simulate the light output response of the BC505 detectors.
- Writes data in exactly the same format as from real experiments.

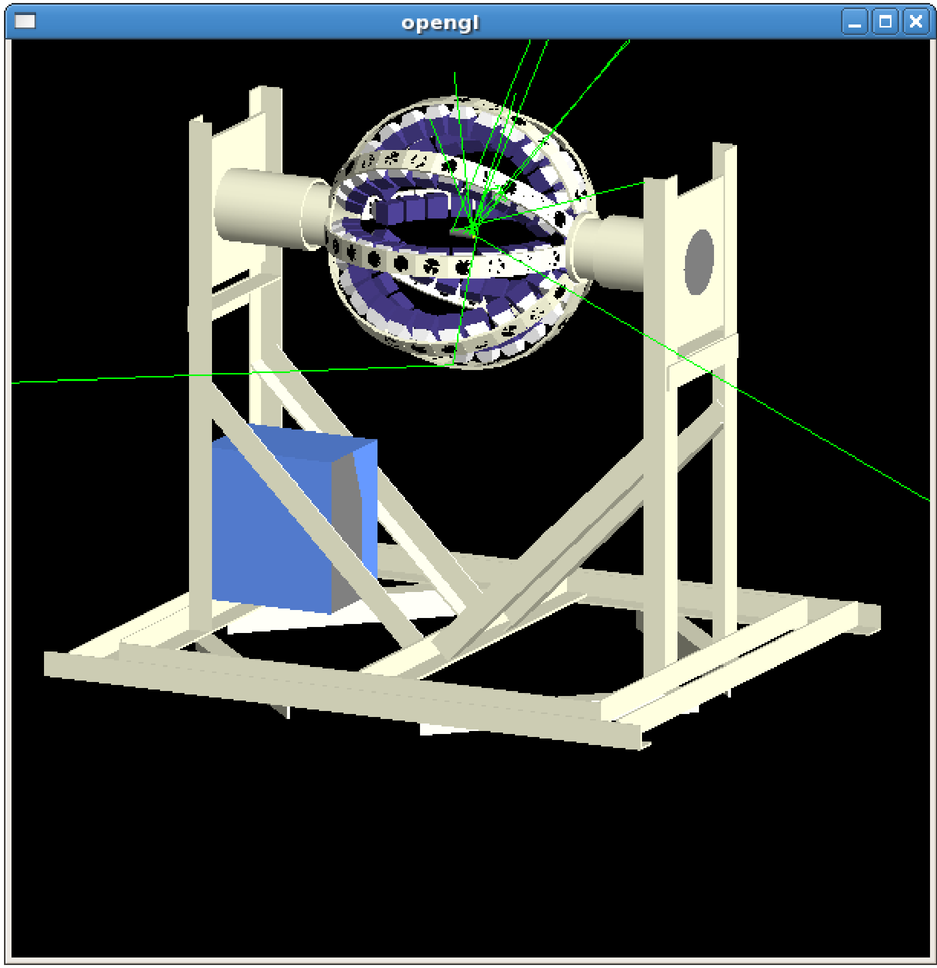

GDH Sum Rule

- Blowfish was originally built for a direct measurement of the Gerasimov-Drell-Hearn (GDH) sum rule for the Deuteron.
- Connects an energy weighted integral of spin-polarized photo-absorption cross sections with the anomalous magnetic moment of the target.
- Based on very general principles: causality, unitarity, gauge and Lorentz invariance.

$$\int_0^\infty \left(\sigma^P(k) - \sigma^A(k)\right)\frac{dk}{k} = 2\pi^2 \alpha S_t \left(\frac{\kappa_t}{M_t}\right)^2$$

σ^P and σ^A	Total inelastic photon cross sections with the target spin and the circularly polarized photon helicity are parallel (P) and antiparallel (A).
κ_t	Anomalous magnetic moment of target.
M_t	Mass of target.
S_t	Target Spin

GDH Sum Rule

Target	Threshold	κ	$\int$GDH
Proton	$k_\pi \approx$ 145 MeV	1.79	204.0 μb
Neutron	$k_\pi \approx$ 145 MeV	–1.91	232.0 μb
Deuteron	$k_d \approx$ 2.2 MeV	–0.14	0.6 μb

Impulse approximation argument suggests:

$$\int_{k_d}^{k_\pi} GDH_{deuteron} \approx -436\ \mu\text{b}$$

GDH Sum Rule

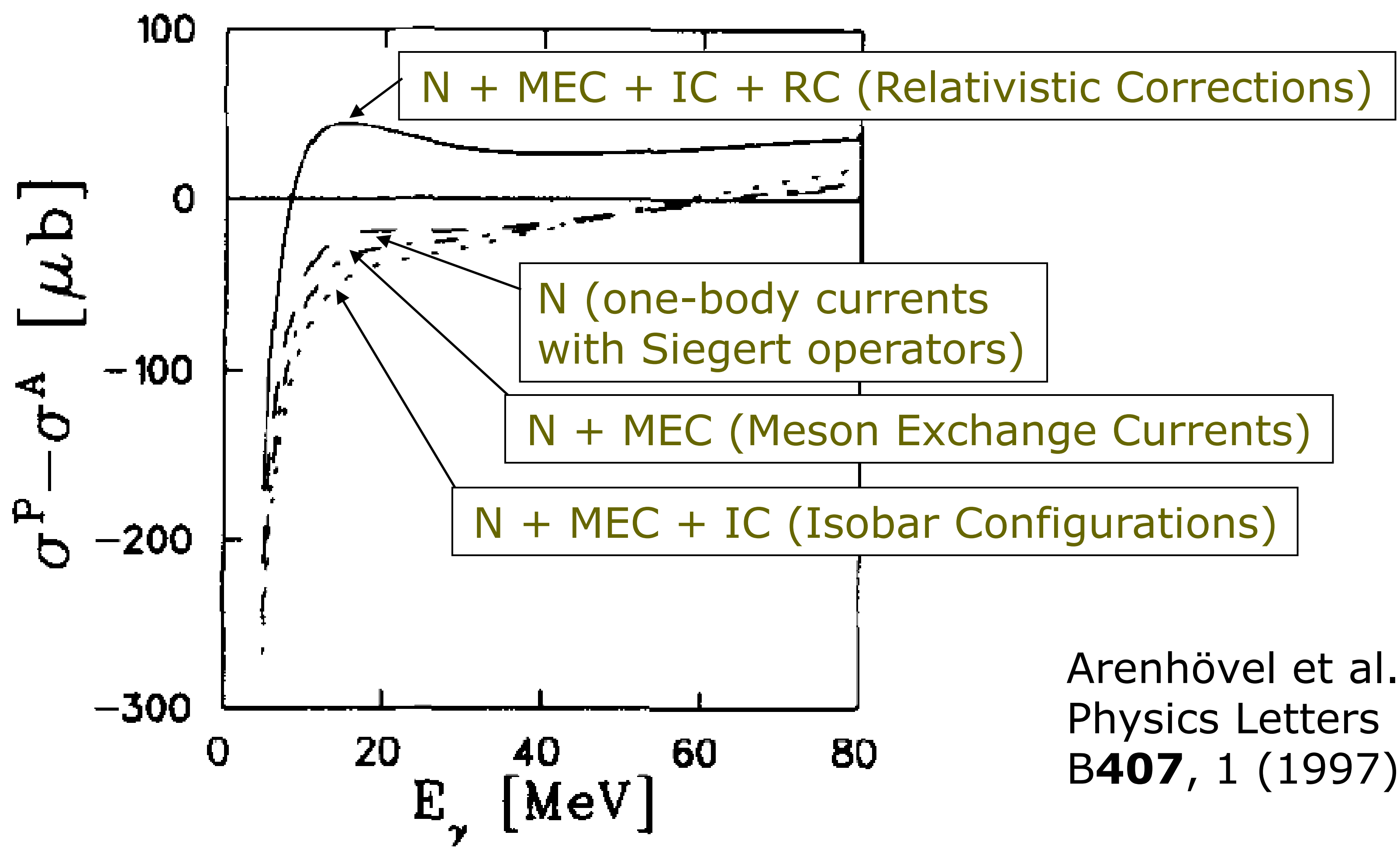

Arenhövel et al. Physics Letters B**407**, 1 (1997).

GDH Sum Rule

- Low energy region ideally suited to HIGS.
- Precision absolute cross sections are needed
  - GDH sum depends on the difference between two absolute cross sections. $(\sigma^P - \sigma^A)$
- Polarized deuterium target (HIFROST) is being installed now.
- Measurements will begin early 2013.

Photon Flux Monitor

- HIGS beam is not continuous.
  - Pulsed at 5.58 MHz (180 ns between bunches)
- A direct counting photon detector with an efficiency known to better than 2% has been designed and commissioned.
  - Low efficiency
    - 1 – 2 %
  - Very stable efficiency
    - Insensitive to small changes in gain
  - Wide energy range
    - 5 – 100 MeV
  - Wide photon flux range
- Now in regular use at HIGS

Photon Flux Monitor

- 5 thin (~1 mm) scintillator paddles
- Detects recoil electrons and positrons from Compton scattering and pair production from a thin Al radiator.
- Described well with a GEANT4 simulation.
- Gains can be monitored by sampling paddle spectra.

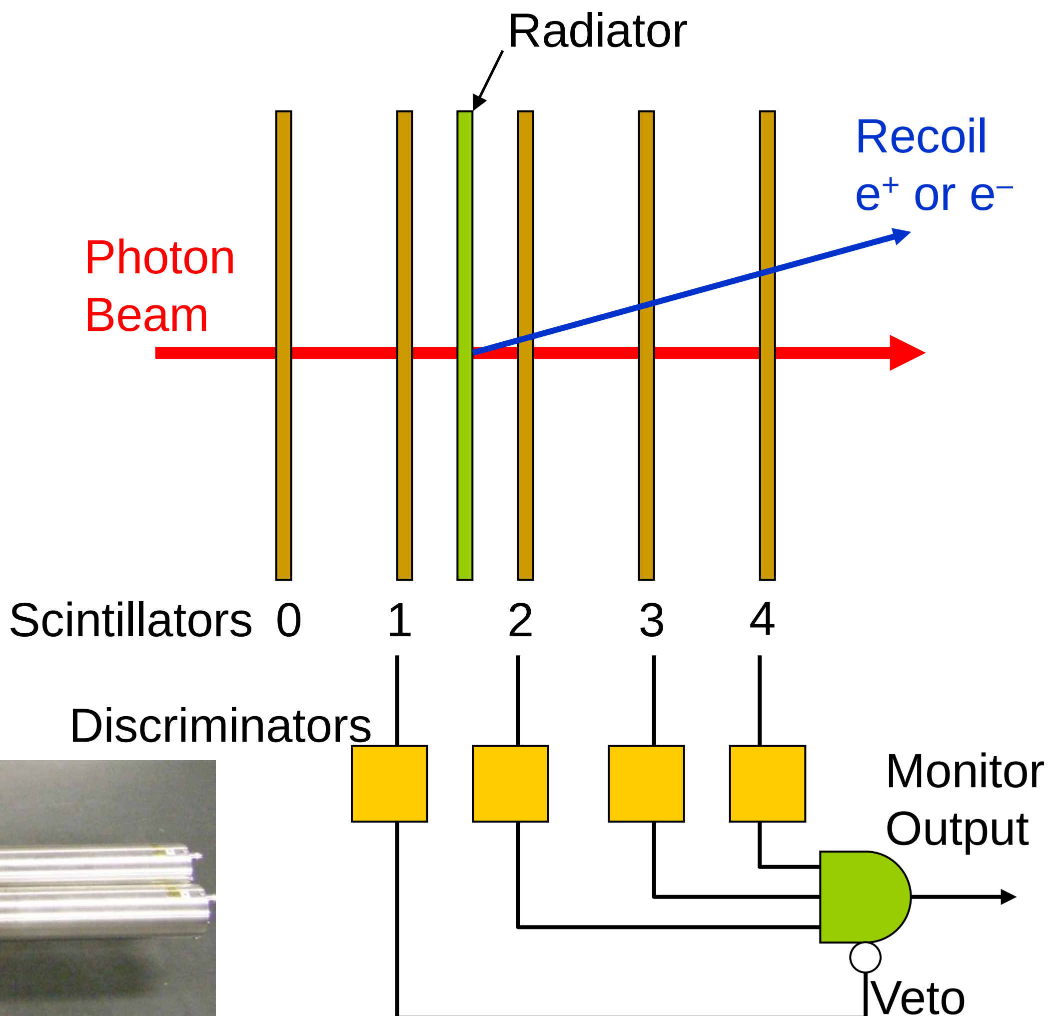

Photon Flux Monitor

- Data compared to GEANT4 simulation

Coincidence of paddles 0, 1 and 2.
Used for determining gain and threshold of paddle 1.

Coincidence of paddles 2, 3 and 4 in anticoincidence with paddle 1.

Black – Measured
Red – Simulation

Threshold

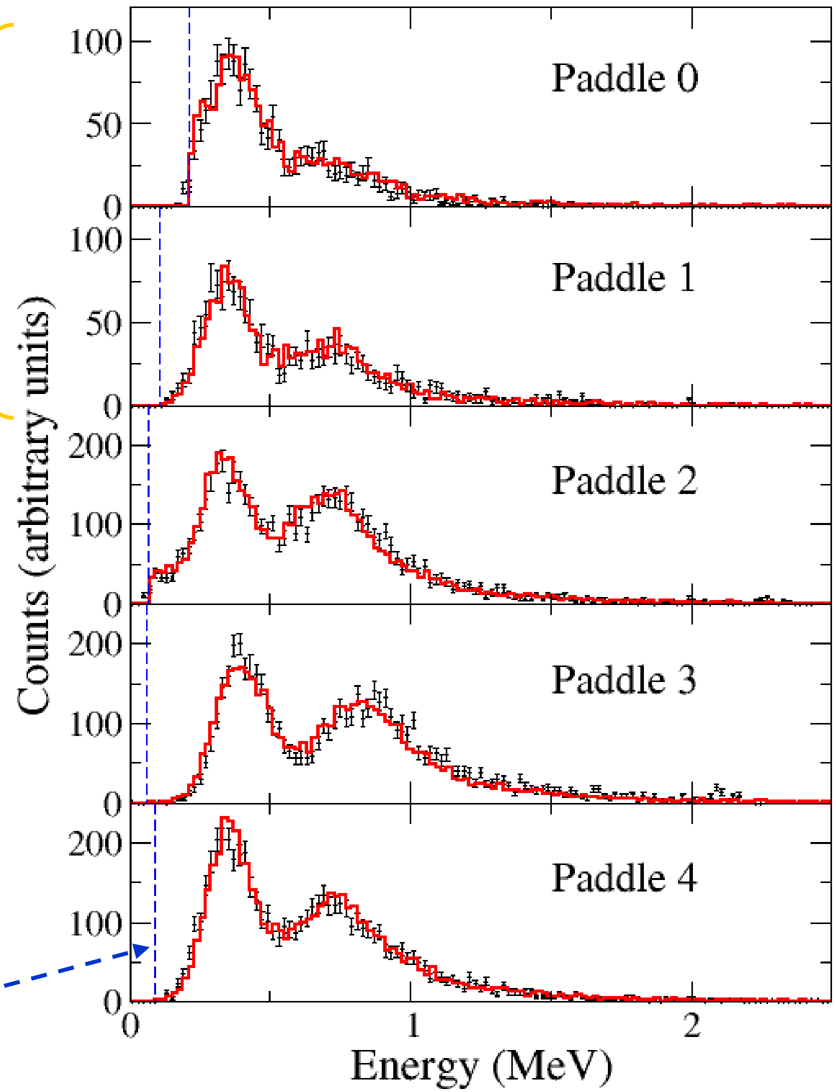

Photon Flux Monitor

- We do not rely on the simulation to predict efficiency.
- Inter-calibrated with a large NaI detector.
  - Regularly during a measurement.

$$N_{\gamma} = f_{Calib} N_{Monitor}$$

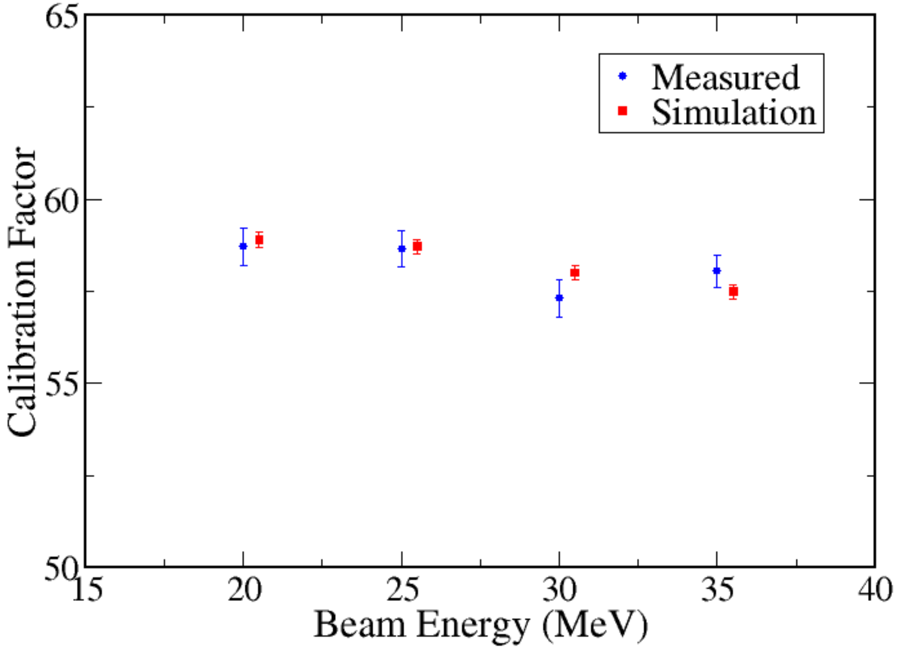

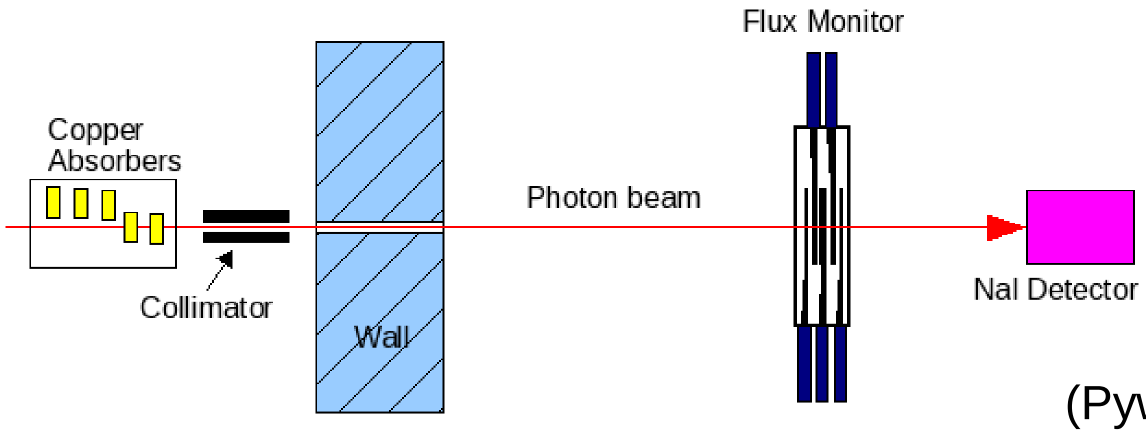

- Can determine f_{Calib} to better than 2%.

(Pywell et at. NIM A 606 (2009) 517)

Photon Flux Monitor

- There are only a few photons in each bunch (bunch rate 5.58 MHz)
- At high photon rates there is chance that more than one photon can trigger the Flux monitor – but only one can be counted per bunch.
- A simple correction can be made using Poisson statistics and using the measured rates in veto paddle.
- Operation of the flux monitor has now been verified in several experiments.

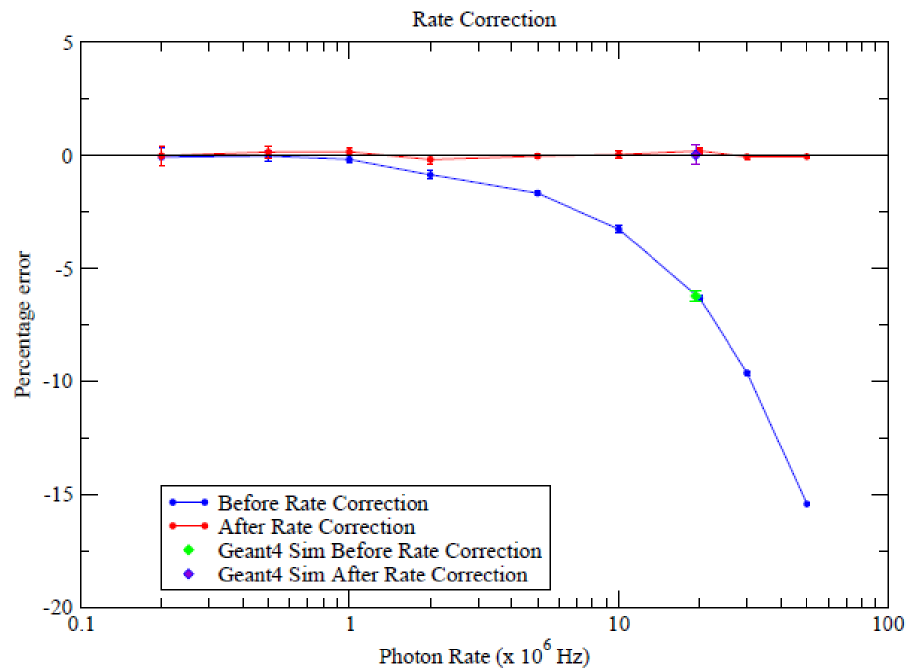

Detectors

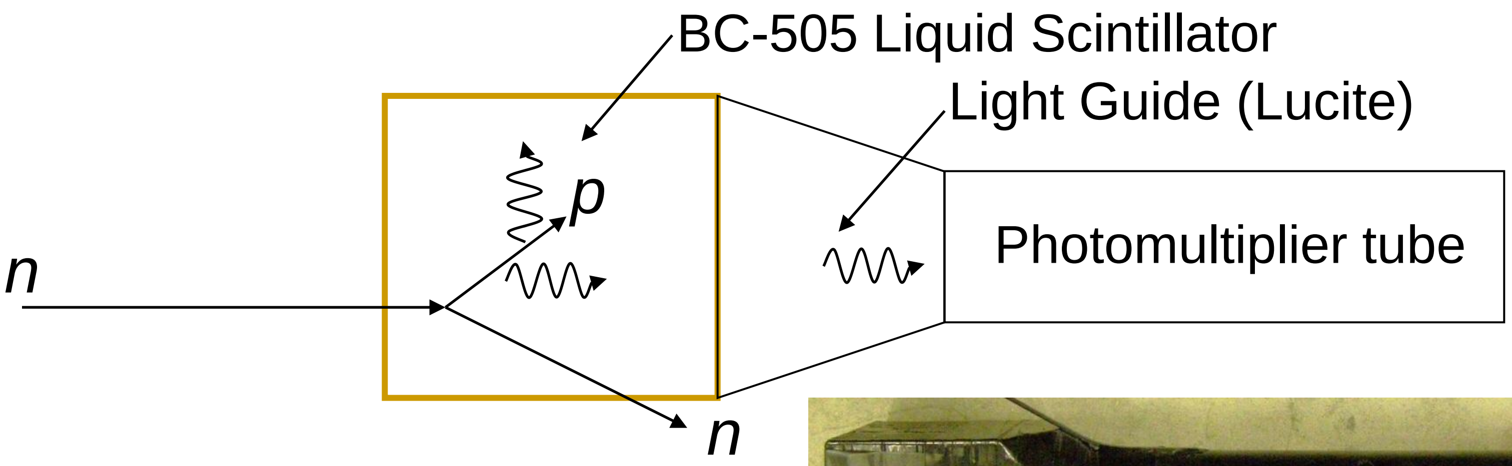

- Neutrons are detected by recoil charged particles in the BC-505 liquid scintillator (mostly protons).

Detectors

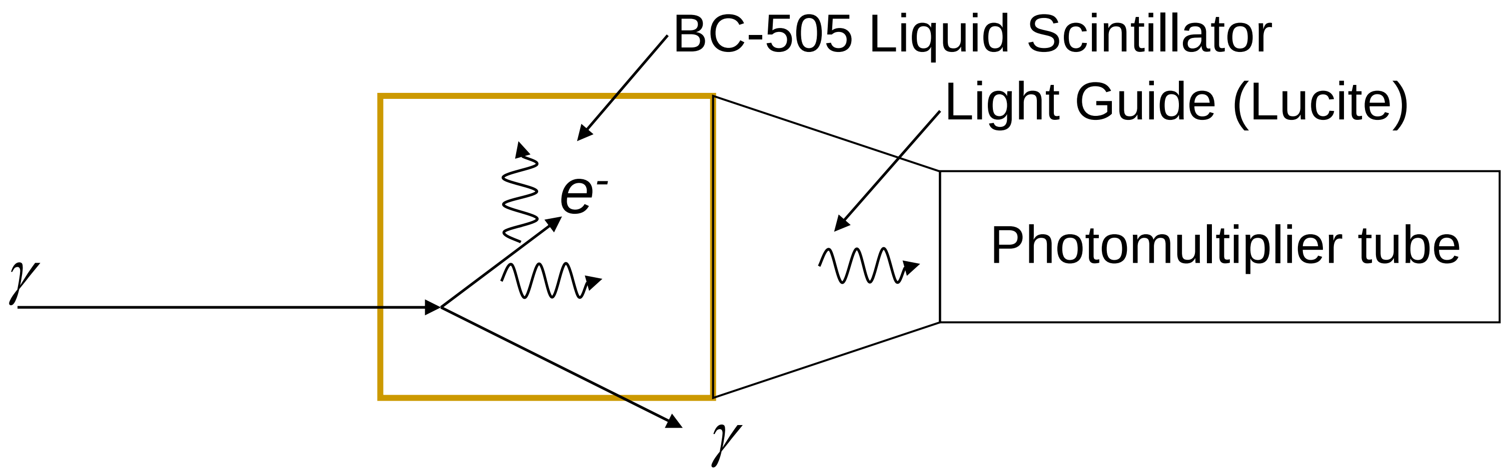

- The detectors are also sensitive to gamma-ray photons through Compton scattering.
- We calibrate the detector with radioactive sources with known energy γ-rays.
- During an experiment we need to separate neutrons against a background of γ-rays.

Pulse Shape Discrimination

- We use pulse shape discrimination to tell the difference between recoil protons (neutrons) and recoil electrons (photons).
- Because of the different way electrons and protons deposit energy in the BC-505, the resulting scintillation light has a different time structure.

Signal from the photomultiplier:

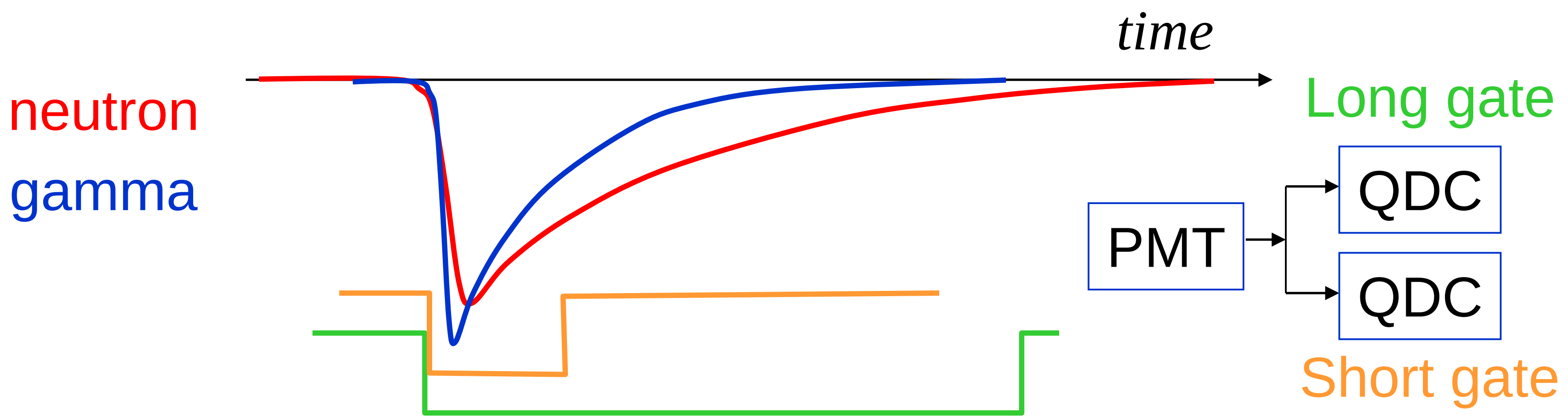

Pulse Shape Discrimination

(Long gate) – (Short gate) ⇒ PSD parameter

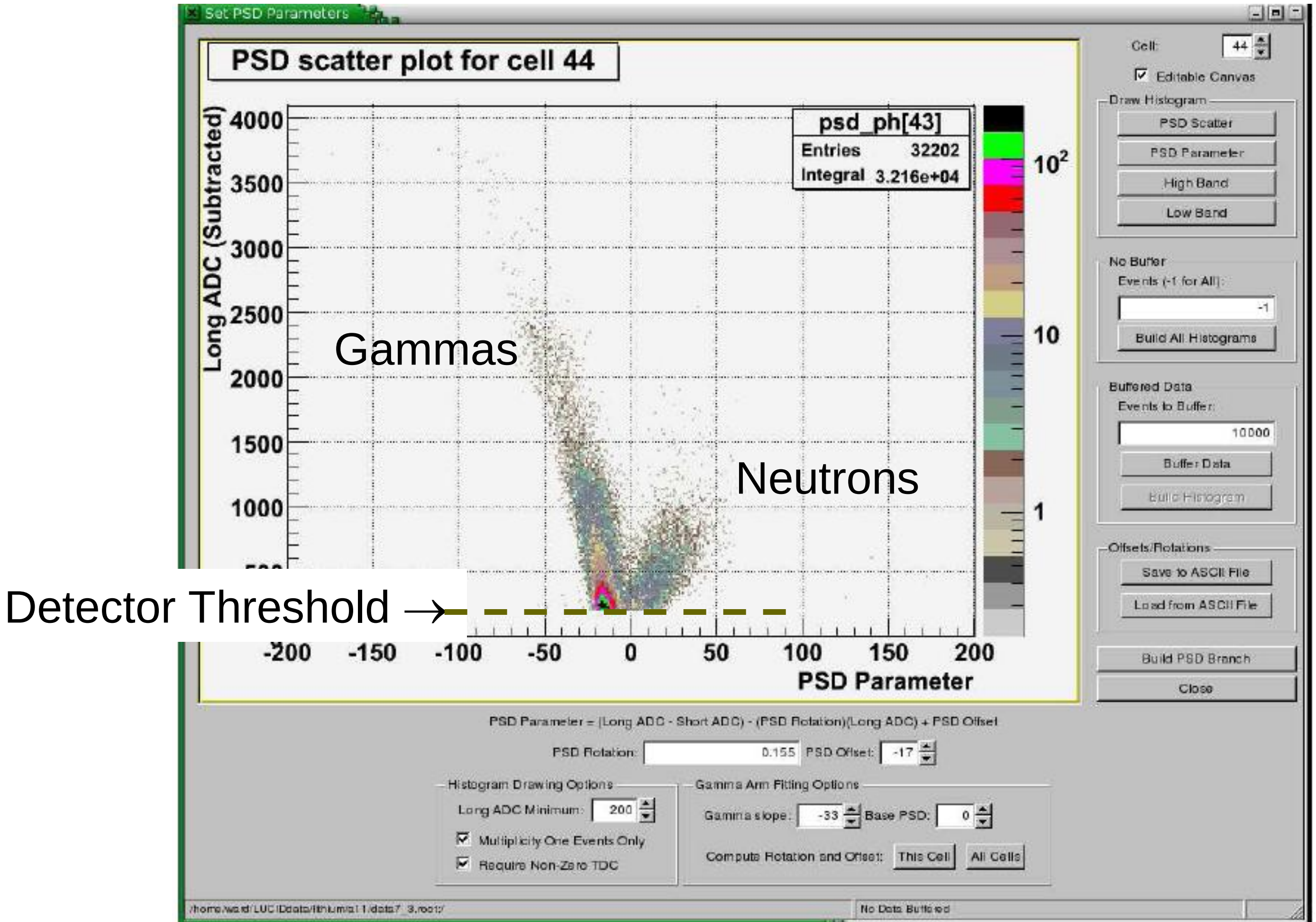

Time of Flight

- We can use time-of-flight to reject the prompt gamma rays from beam photons Compton scattered from the target and other materials.
- The Compton scattered gamma rays can be used to set the zero for the time-of-flight of the neutrons.

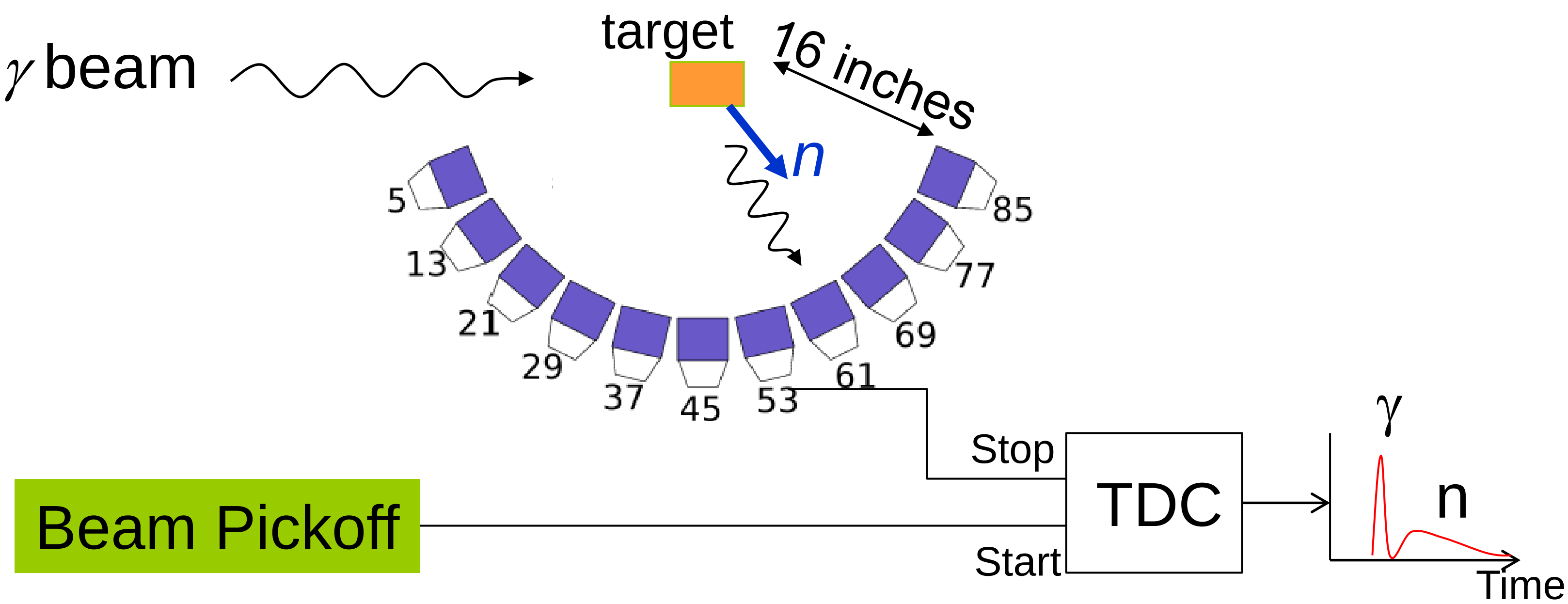

Time of Flight

- From the time-of-flight the neutron energy can be determined.
- e.g. With a D_2O target
  - the expected neutron energy can be calculated from the incident photon energy and the deuterium kinematics.
  - the difference between the measured neutron energy and the expected neutron energy is plotted.

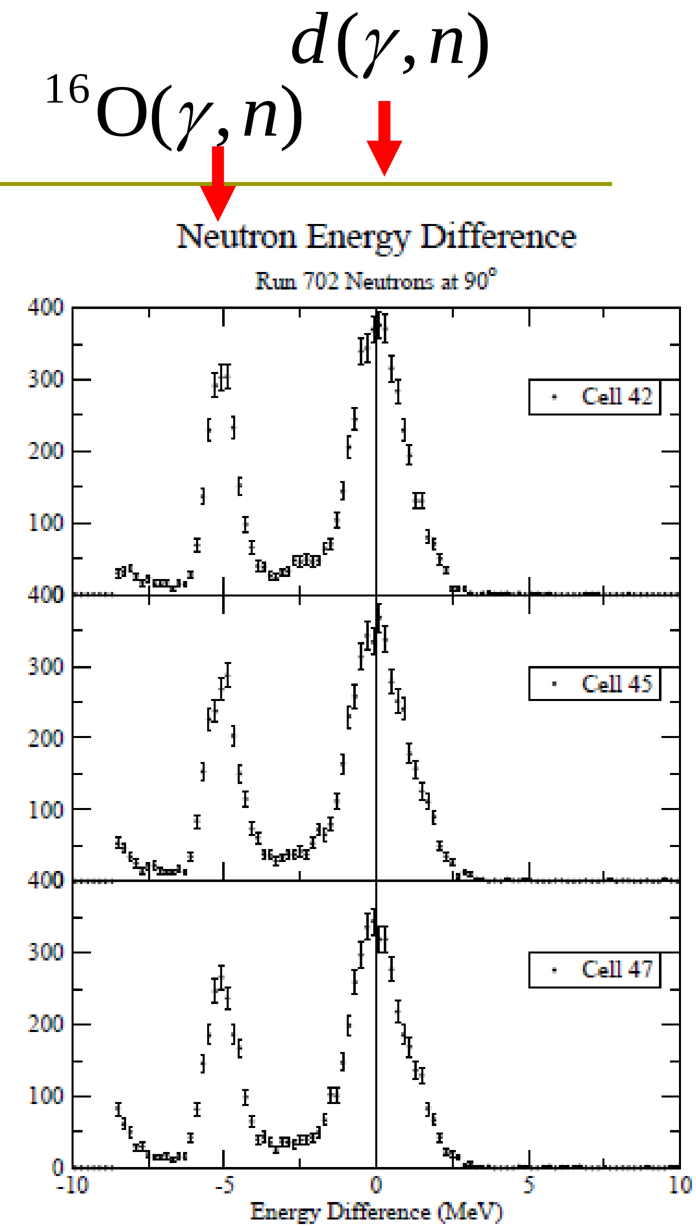

Detector Efficiency

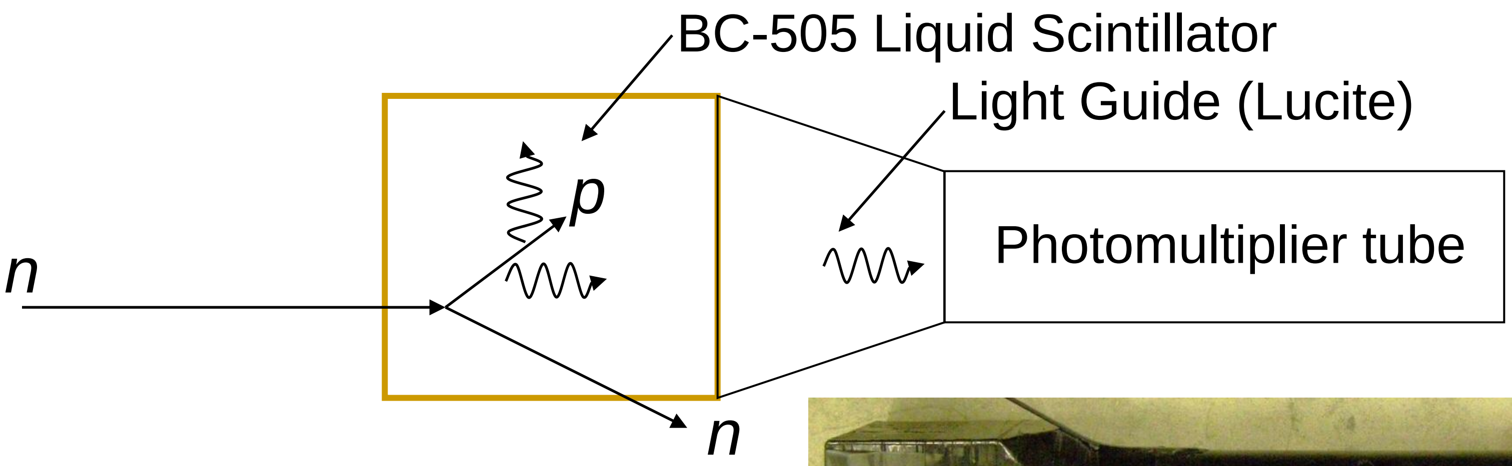

- For a given neutron energy there is a distribution of recoil proton energies up to the neutron energy.

Detector Efficiency

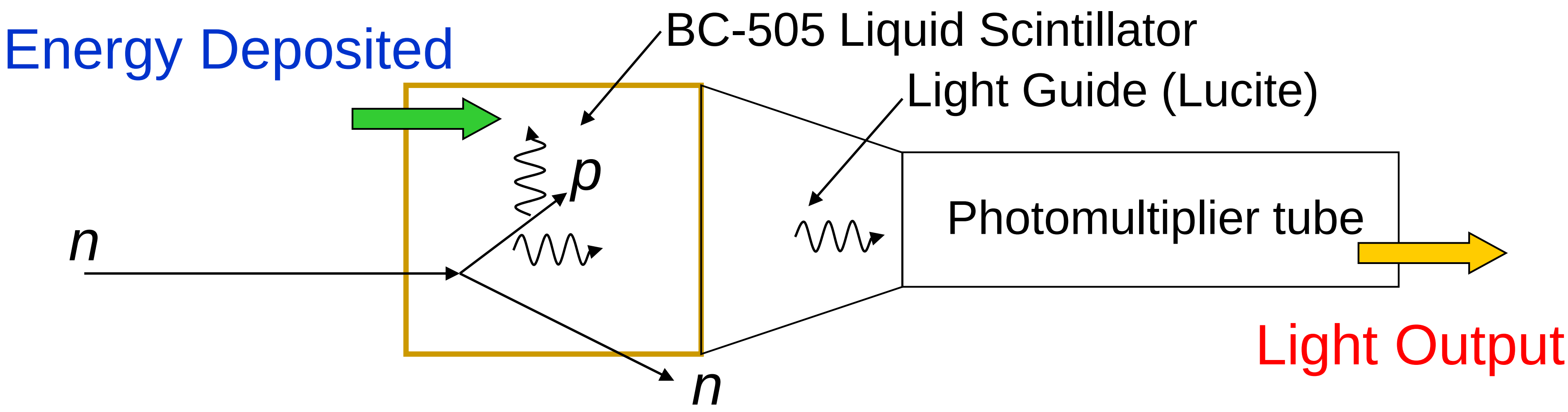

- The relationship between energy deposited and light output is not linear.
- Depends on particle type.

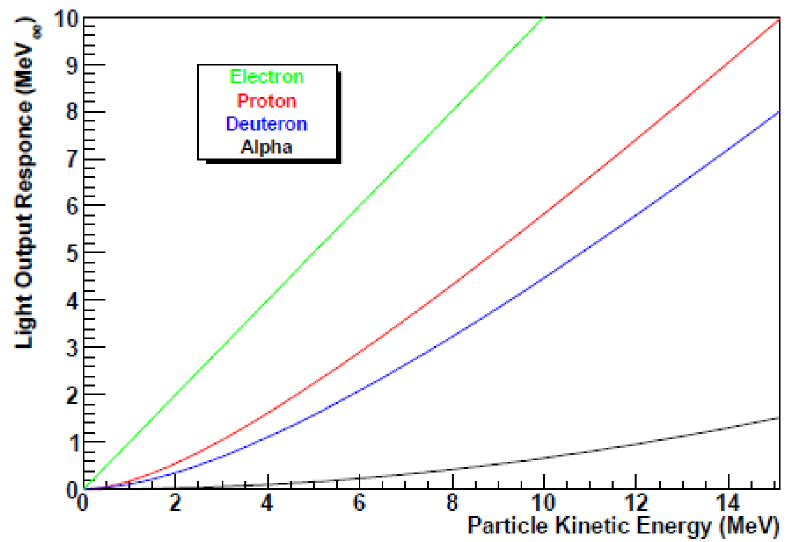

Light Output Response of BC-505

- The scintillation light output is in general not simply proportional to the particle energy.
- Understanding the light output is vitally important to simulating the detector response accurately so that the efficiency can be calculated.

Light output spectrum from 9.8 MeV "tagged" neutrons from the $\pi^- p \rightarrow n\gamma$ reaction, measured at TRIUMF.

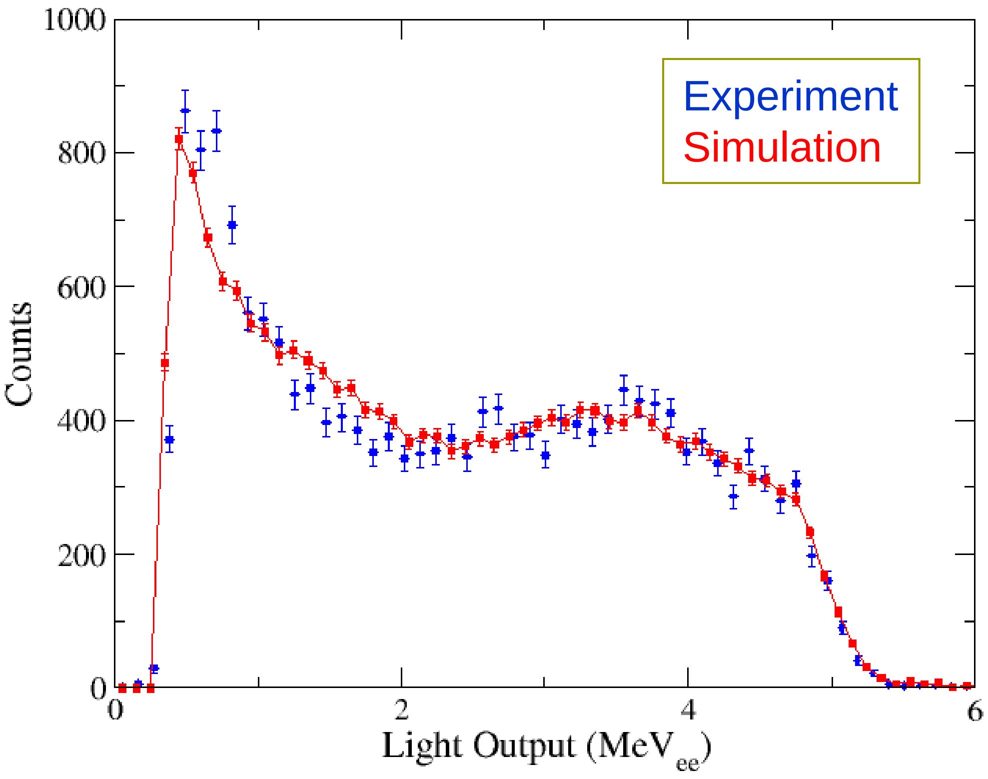

Light Output Response of BC-505

- Excellent fits to measurements have been obtained using the Chou parameterization.

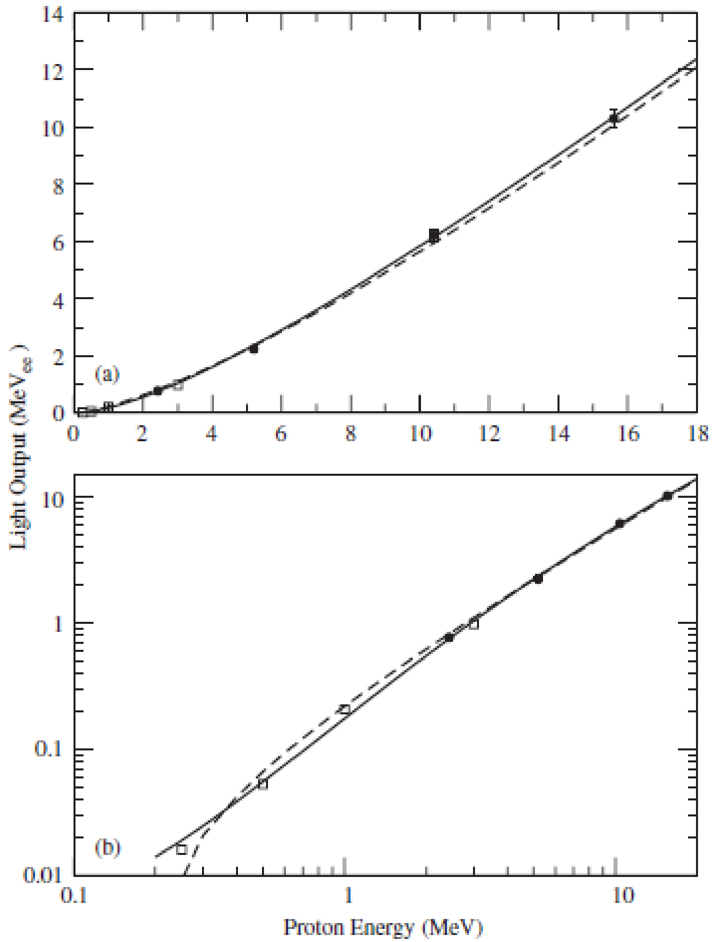

Light output for a particle of energy E stopping in a material with range R.

$$L(E) = \frac{dE/dx_{\min}}{f\,(dE/dx_{\min})} \int_0^R f\left(\frac{dE}{dx}\right) dx$$

With,

$$\frac{dL}{dx} \propto f\left(\frac{dE}{dx}\right) = \frac{dE}{dx}\left[1 + kB\left(\frac{dE}{dx}\right) + C\left(\frac{dE}{dx}\right)^2\right]^{-1}$$

Light output response functions have been built into GEANT4.

Pywell et al. NIM A 565 (2006) 725

Detector Efficiency

- The detector efficiency is determined by integrating the light output spectrum from a hardware discriminator threshold (or software threshold)
- This is done through the GEANT4 simulation with the threshold as input.
- It is therefore vitally important to know the gain of a detector.
  - Measured using a radioactive source.
  - But drifts can occur during a measurement period.

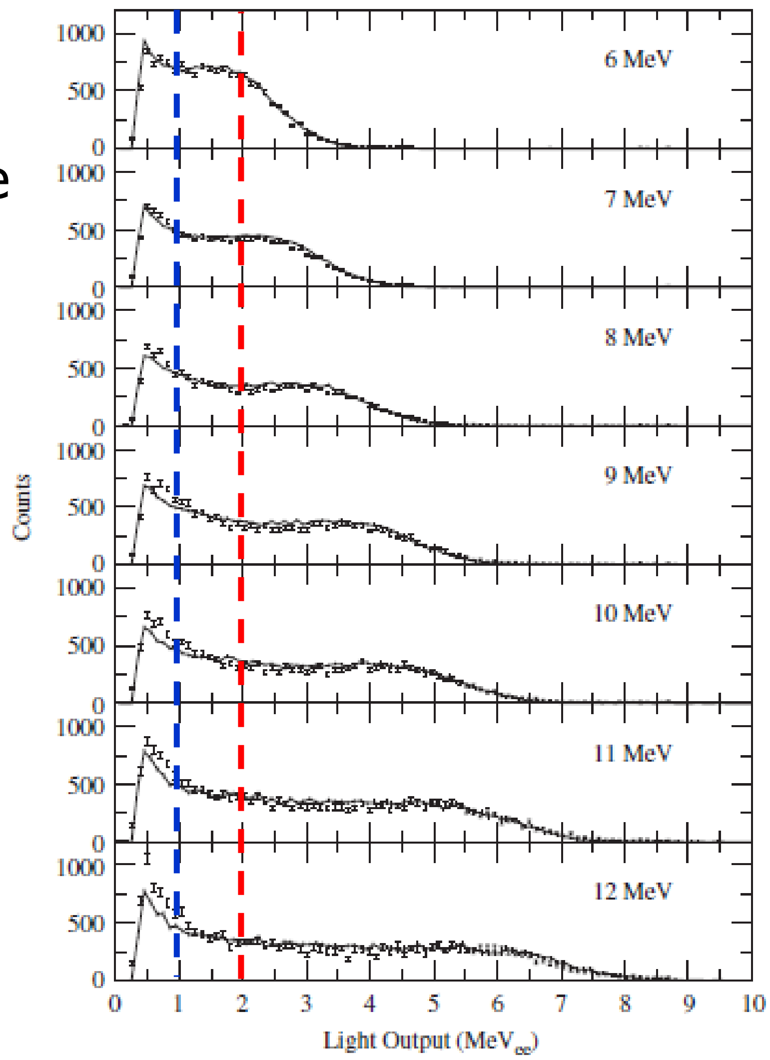

Gain Monitoring System

- LED light pulser with a Fiber optic light distribution system.
- Monitored with a GSO scintillator and radioactive source.
- Does not depend on the stability of any components.

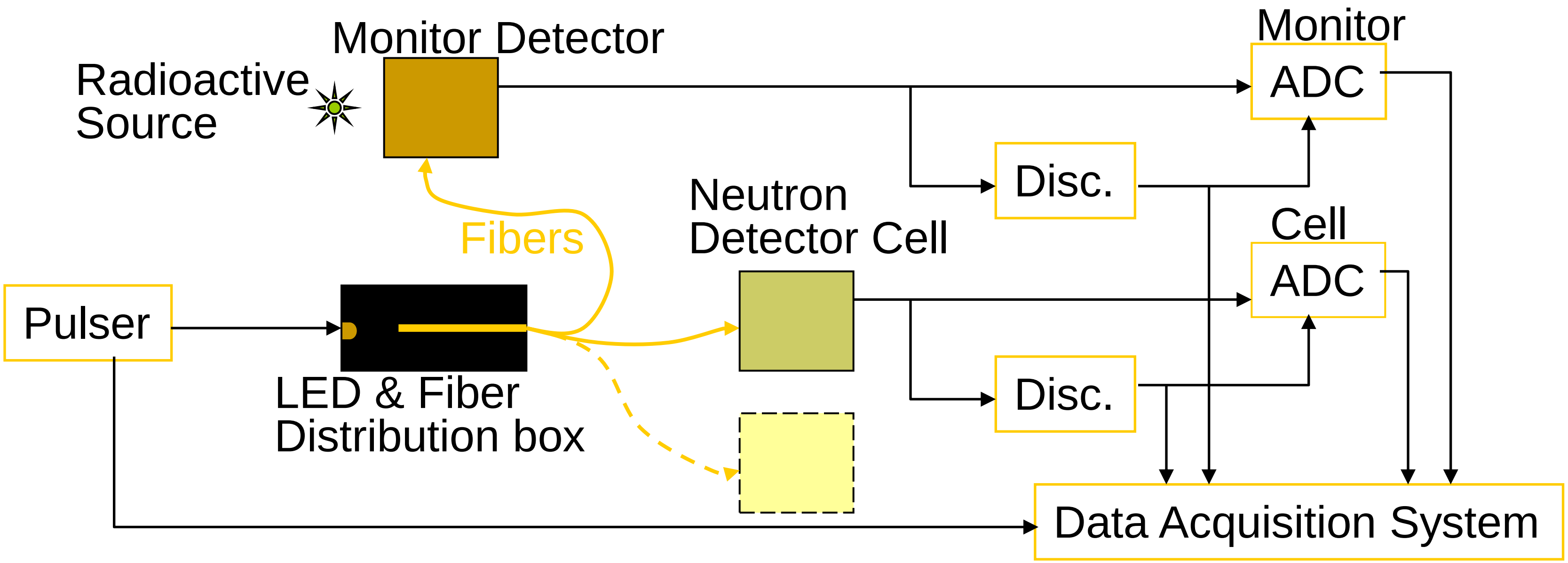

Bewer et al. NIMA 608 (2009) 417

Cross Section

e.g. Deuterium – only one reaction channel

- We parameterize the cross section in terms of associated Legendre functions
  - For linearly polarized photons

$$\frac{d\sigma}{d\Omega}(\theta,\varphi) = \frac{\sigma}{4\pi}\left[1+\sum_{k=1}^{\infty} a_k P_k^0(\cos\theta) + \sum_{k=2}^{\infty} e_k P_k^2(\cos\theta)\cos 2\varphi\right]$$

θ = centre-of-mass polar angle w.r.t. beam

φ = azimuthal angle w.r.t. beam polarization

  - For circularly polarized photons

$$\frac{d\sigma}{d\Omega}(\theta) = \frac{\sigma}{4\pi}\left[1+\sum_{k=1}^{\infty} a_k P_k^0(\cos\theta)\right]$$

  - We find $k \leq 4$ sufficient.

Detector Efficiency

- The parameterisation is used as input to the GEANT4 simulation to find the response for each cell.
- The simulation can be used to find the response for each cell to each Legendre function.
- A fit is done to the measured neutron yield in all the cells to determine the parameters.
- The parameterization can be integrated to get the total cross section.
- The result is total cross sections and θ and φ angular distributions.

Deuterium Photodisintegration

- 20 MeV – Example of parameter fit. Circularly polarized photons

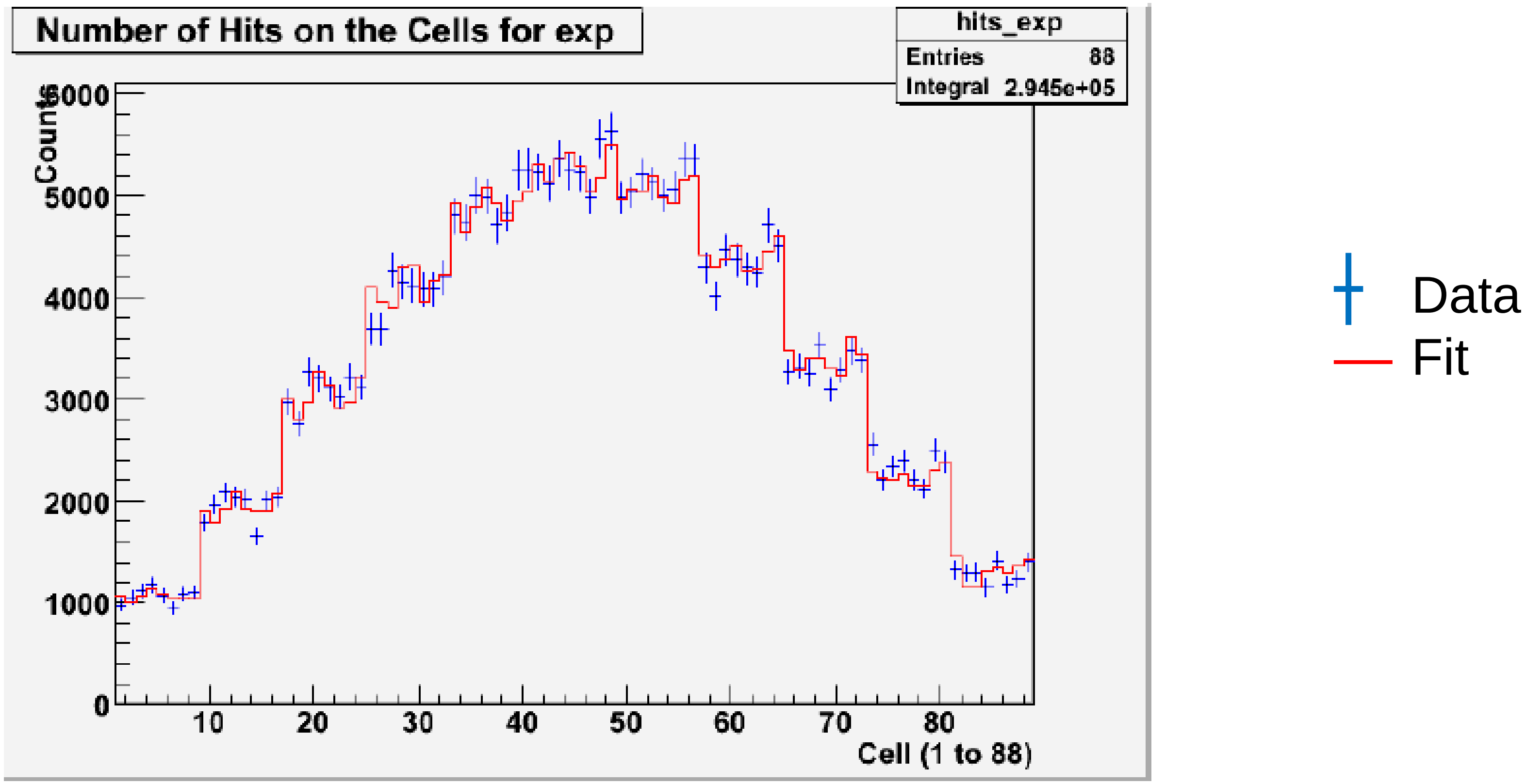

S. Kucuker, PhD Dissertation

Deuteron Photodisintegration

a_1

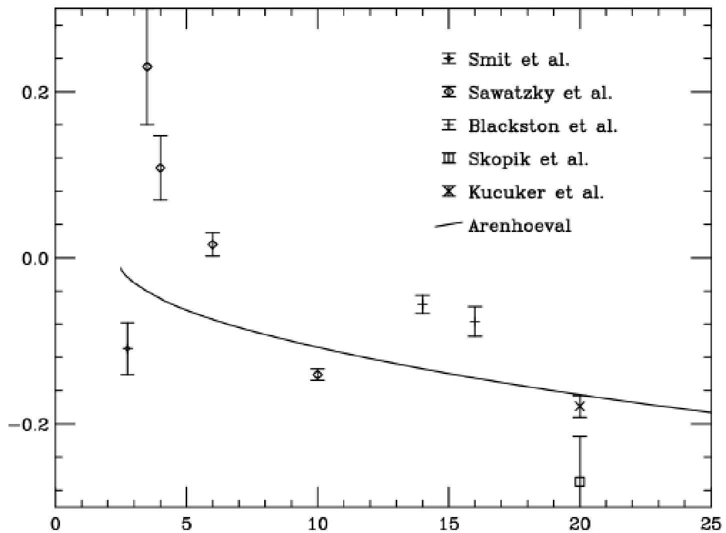

a_2

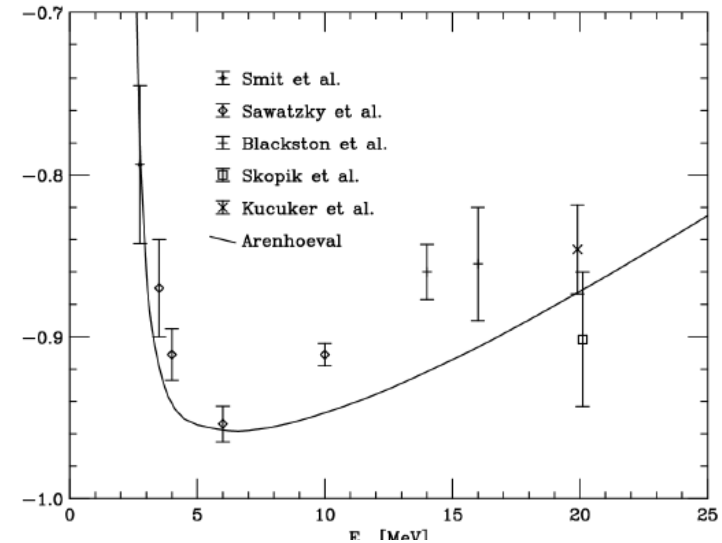

a_3

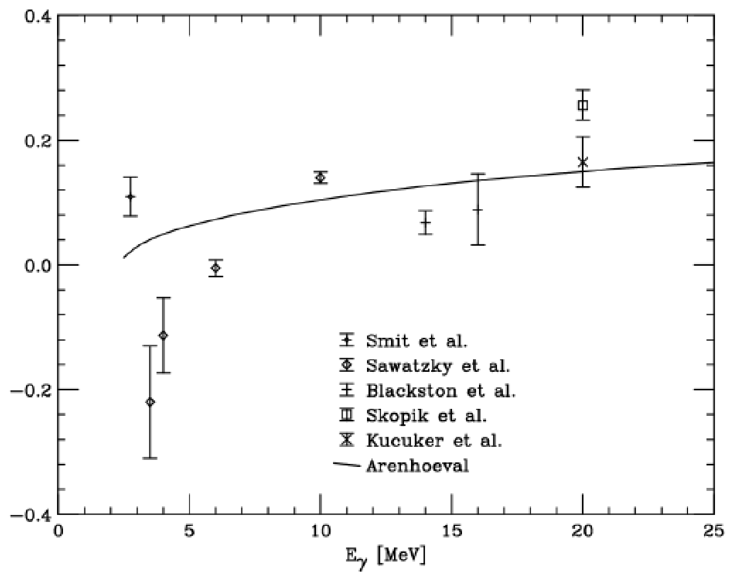

a_4

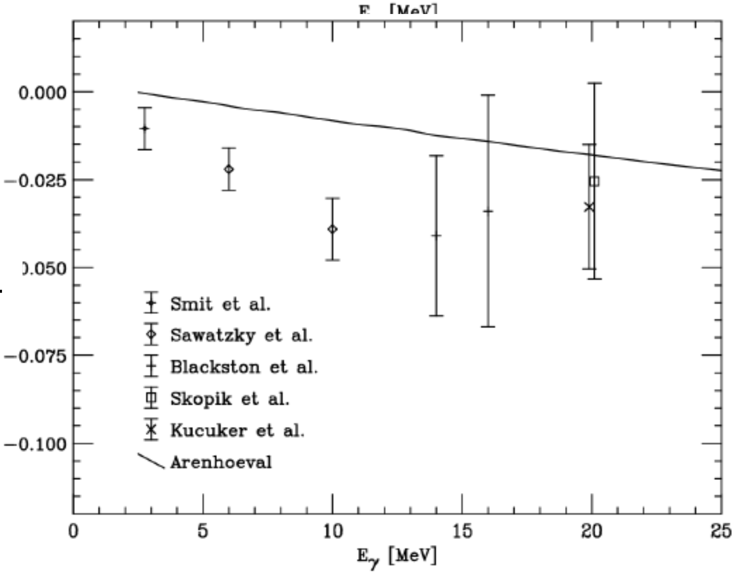

Deuteron Photodisintegration

$P_{y'}$ = Neutron spin polarization

$$d(\gamma,\vec{n})p$$

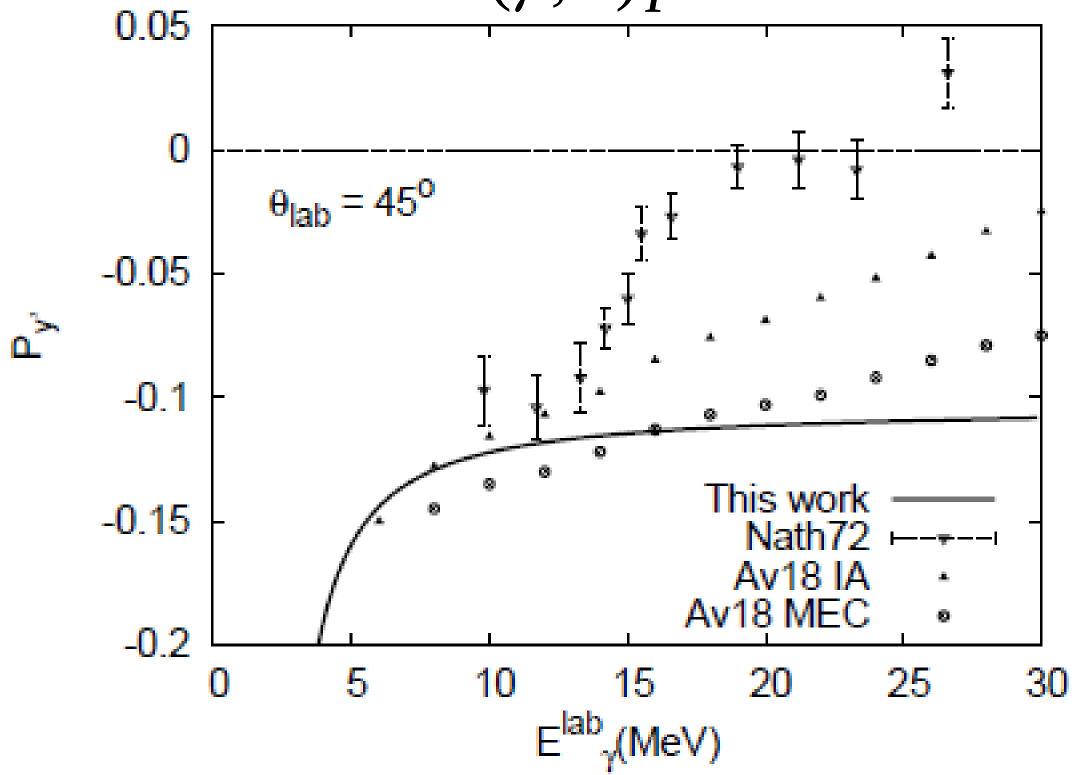

We are proposing to measure

$$d(\vec{\gamma},\vec{n})p$$

for E_γ = 8-16 MeV for a range of neutron angles.

Arenhövel providing theoretical support.

S-I, Ando et al. arxiv:nucl-th/1103.4434v2 (2011)

^{4}He Photoneutron Cross Section

- We will measure $^4He(\gamma,n)$ between 20 and 40 MeV.
- High pressure gas target has been constructed and tested by collaborators at Kharkov Institute, Ukraine.
- He cell is a stainless steel can inside a H_2 filled tube
- Designed with a safety factor of 3

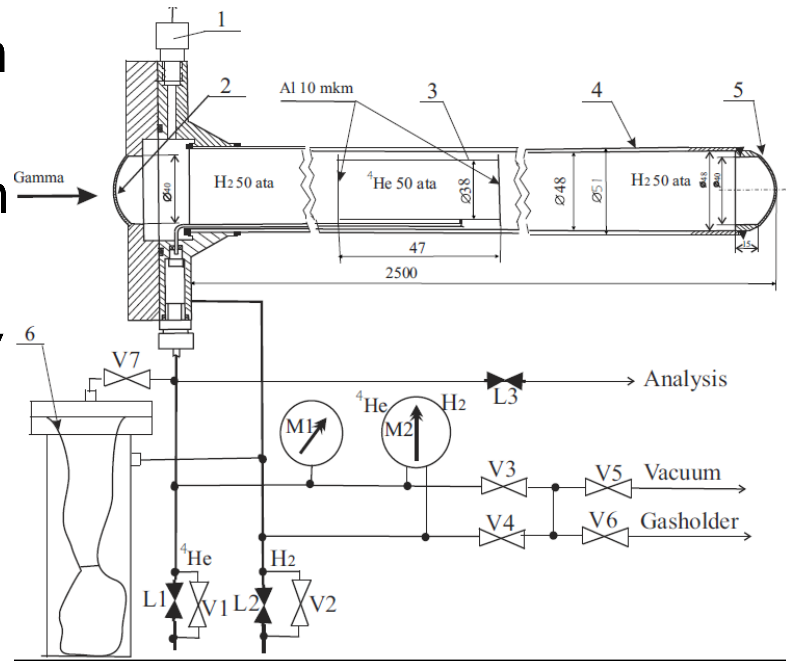

^{4}He Photoneutron Cross Section

- Geant4 simulations show that
  - at detector thresholds where we have good PSD
  - the gain tracking system can ensure that detector efficiencies are sufficiently well know that
  - the overall detector efficiencies can be know to ~2%
- Then including the photon counting uncertainty we can expect cross sections to within ~3%

Measurements with ^{6}Li and ^{7}Li

- Measurements were made using ^{6}Li, ^{7}Li(nat), and Blank targets.
- Linear polarized photons at 8, 9, 10, 11, 12, 13, 15 and 15.6 MeV.
- Circularly polarized photons at 20, 25, 30 and 35 MeV.
- Two blowfish array orientations were used at most energies to quantify systematics.

Teflon target container

^{6}Li

- One detector cell, θ = 90°, E_{γ} = 13 MeV
- Neutron energy distribution obtained from time-of-flight
- Red – φ = 0° wrt $\vec{\gamma}$
- Blue – φ = 90° wrt $\vec{\gamma}$

^{5}He → ^{4}He + n
neutrons are isotropic

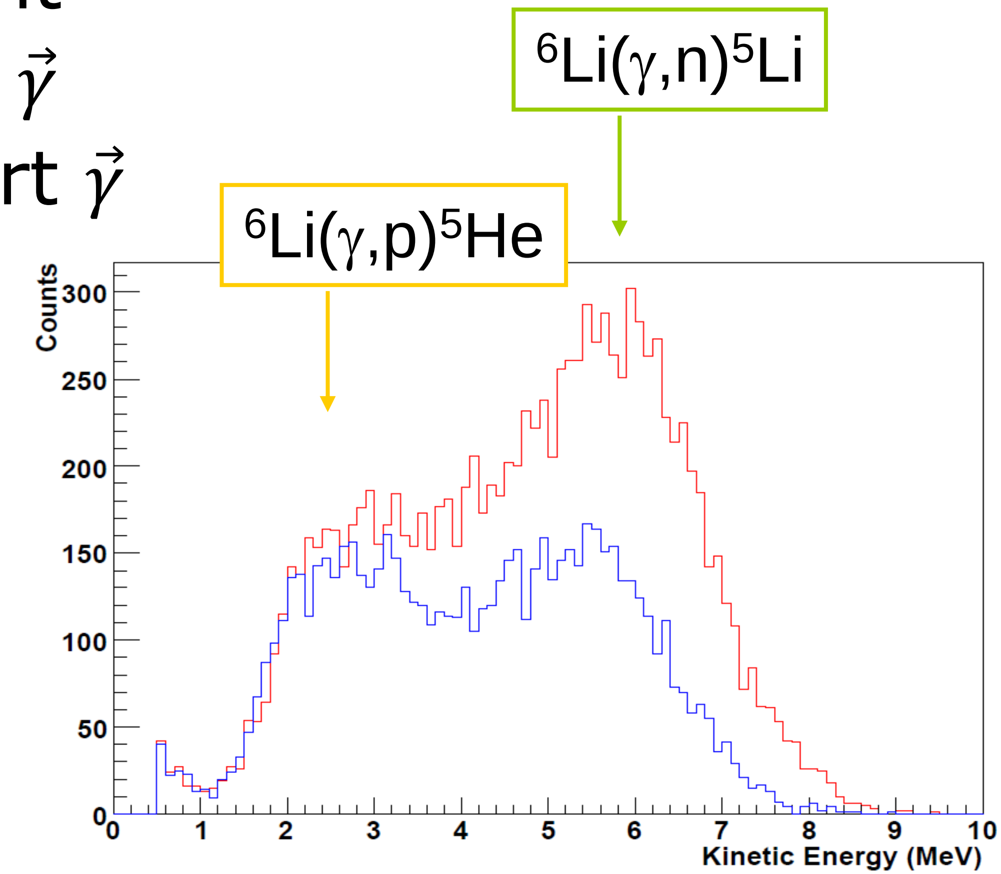

Detector Simulation

- In general there are many reaction channels producing neutrons to consider.
- Each channel is characterized by a different neutron energy spectrum.
- This must be included in the detector response function.

Reaction Channels with neutrons in the final state for ^{6}Li.

Label	Reaction	Threshold (MeV)
(γ, p_0)	$^6\text{Li} + \gamma \rightarrow p + {}^5\text{He(g.s.)} \rightarrow n + p + {}^4\text{He}$	4.6
(γ, n_0)	$^6\text{Li} + \gamma \rightarrow n + {}^5\text{Li(g.s.)}$	5.7
(γ, p_1)	$^6\text{Li} + \gamma \rightarrow p + {}^5\text{He}(1.27) \rightarrow n + p + {}^4\text{He}$	5.9
(γ, n_1)	$^6\text{Li} + \gamma \rightarrow n + {}^5\text{Li}(1.49)$	7.0
(γ, p_2)	$^6\text{Li} + \gamma \rightarrow p + {}^5\text{He}(16.8) \rightarrow n + p + {}^4\text{He}$	21.4
(γ, n_2)	$^6\text{Li} + \gamma \rightarrow n + {}^5\text{Li}(16.9)$	22.6
(γ, p_3)	$^6\text{Li} + \gamma \rightarrow p + {}^5\text{He}(19.1) \rightarrow n + p + {}^4\text{He}$	23.7
(γ, n_3)	$^6\text{Li} + \gamma \rightarrow n + {}^5\text{Li}(19.3)$	25.0

Fitting

- Fit to each neutron detector time-of-flight spectrum after PSD cuts based on the expected neutron energy spectrum for each reaction channel.

Example:

^{6}Li at

E_γ = 20 MeV

Background from atmospheric nitrogen.

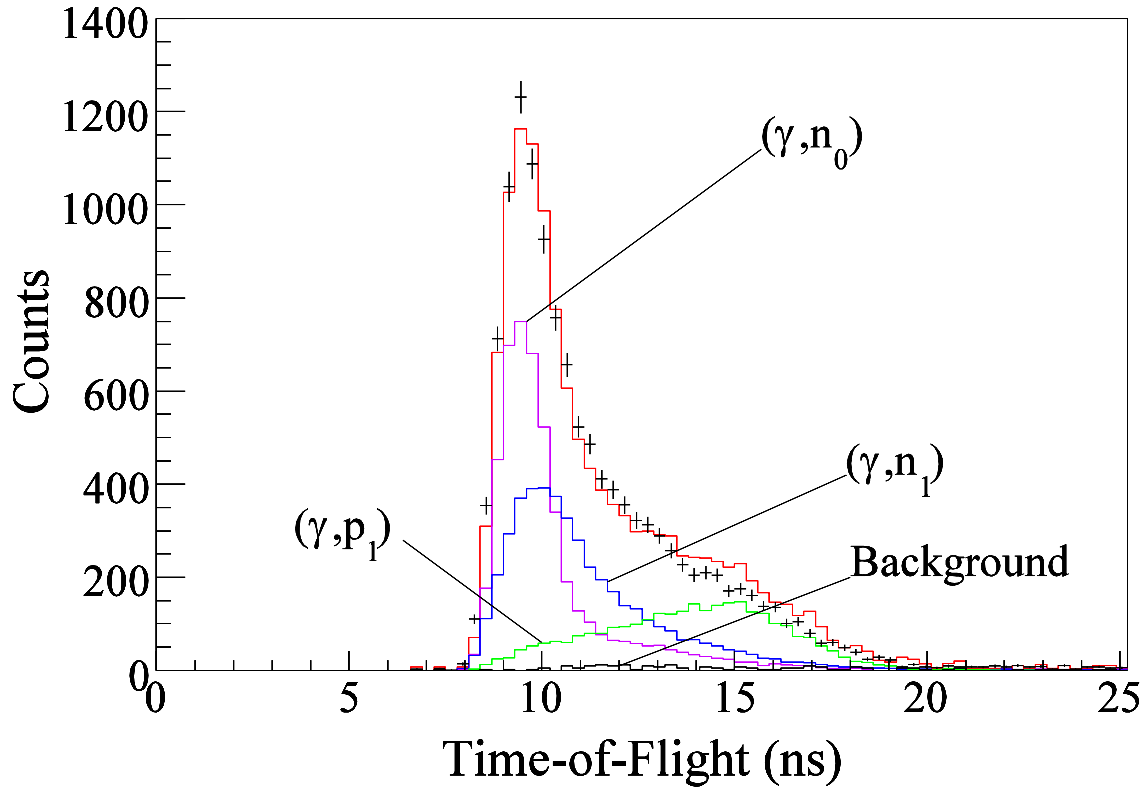

Fitting

- Then, knowing the contribution from each reaction channel in each detector cell we can fit the yields in each cell to determine the differential cross section coefficients.

Example:

^{6}Li at

E_γ = 13 MeV

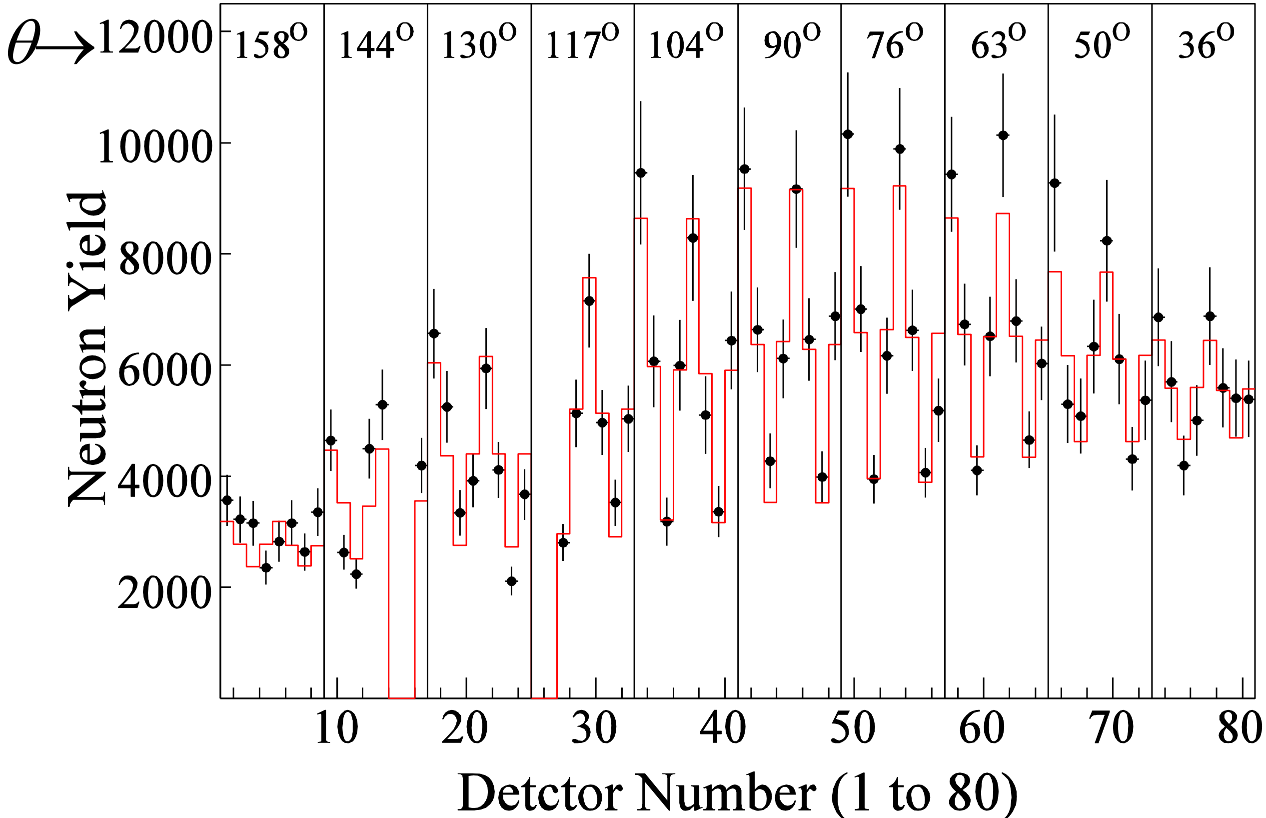

Fitting

- Not all reaction channels contribute significantly at all energies.
- Some reaction channels at some energies have neutron energy distributions that cannot be separated with statistical significance – so they are combined in the fit.
  - e.g. At 20 MeV we can only extract the cross section for $^{6}Li(\gamma,n_0+n_1)$
- Only those coefficients that are needed to accurately describe the cross section, with statistical significance, are reported.
  - e.g. Coefficients a_1, a_2, e_2, e_3 are extracted for the $^{6}Li(\gamma,n_0)$ channel.
  - e.g. Only a_1 Coefficient is statistically significant for the $^{6}Li(\gamma,p_1)$ channel.

^{6}Li and ^{7}Li

- Error bars include systematic uncertainties
- Total uncertainty between

  3 – 5%

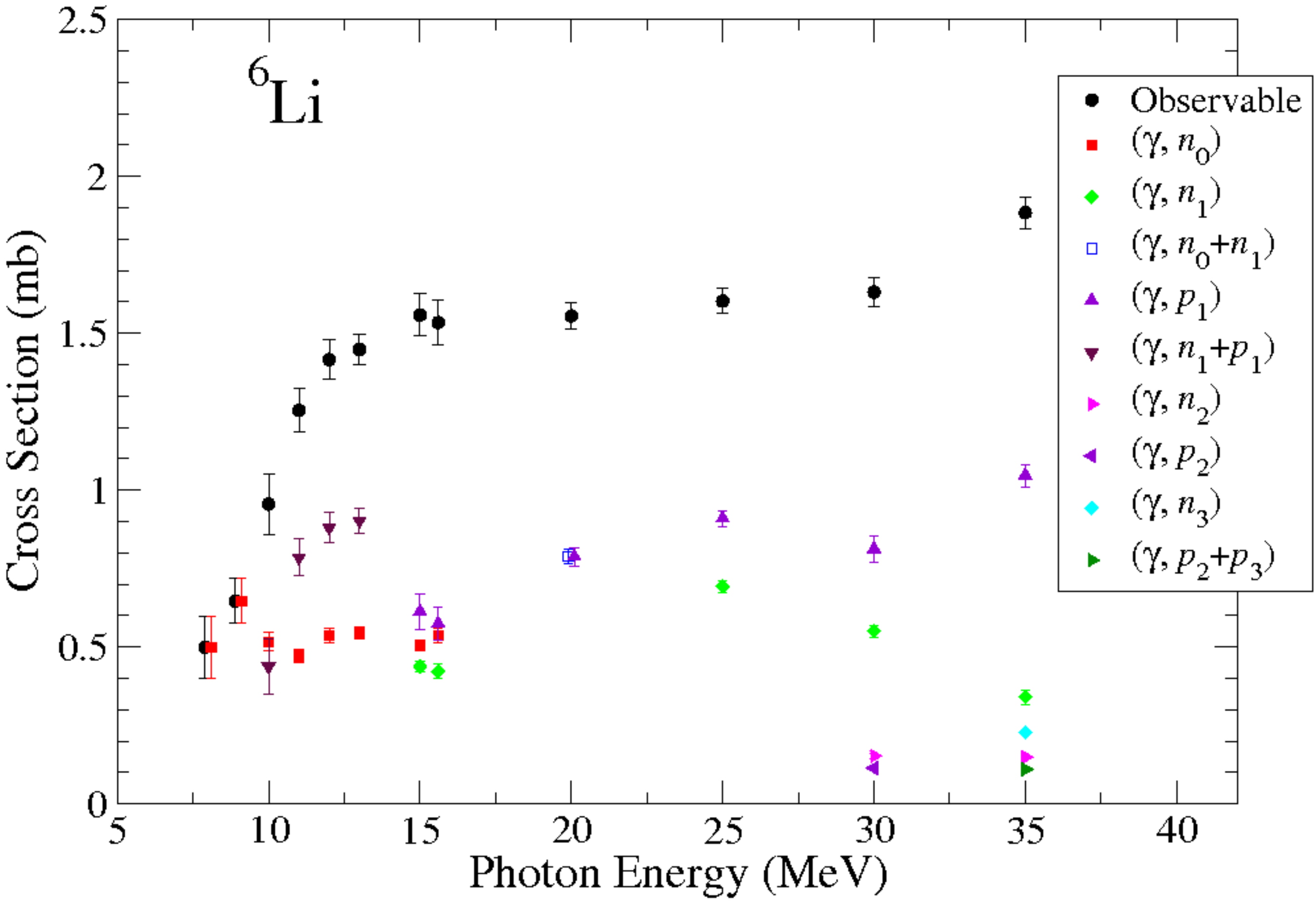

Comparison to Earlier Photoneutron Measurements

- Although the ^{6}Li(γ,p_0) channel produces neutrons, they are of low energy and are below our detector thresholds.
- Previous measurements, such as the quasi-monoenergetic photon measurements of the Livermore group, are sensitive to neutrons of all energies.
- Direct measurements of (γ,p_0) are poor.
- Therefore, to make a comparison, the best we can do is make the assumption that

$$\sigma(\gamma,p_0) = \sigma(\gamma,n_0) \pm 100\%$$

Comparison to Earlier Photoneutron Measurements

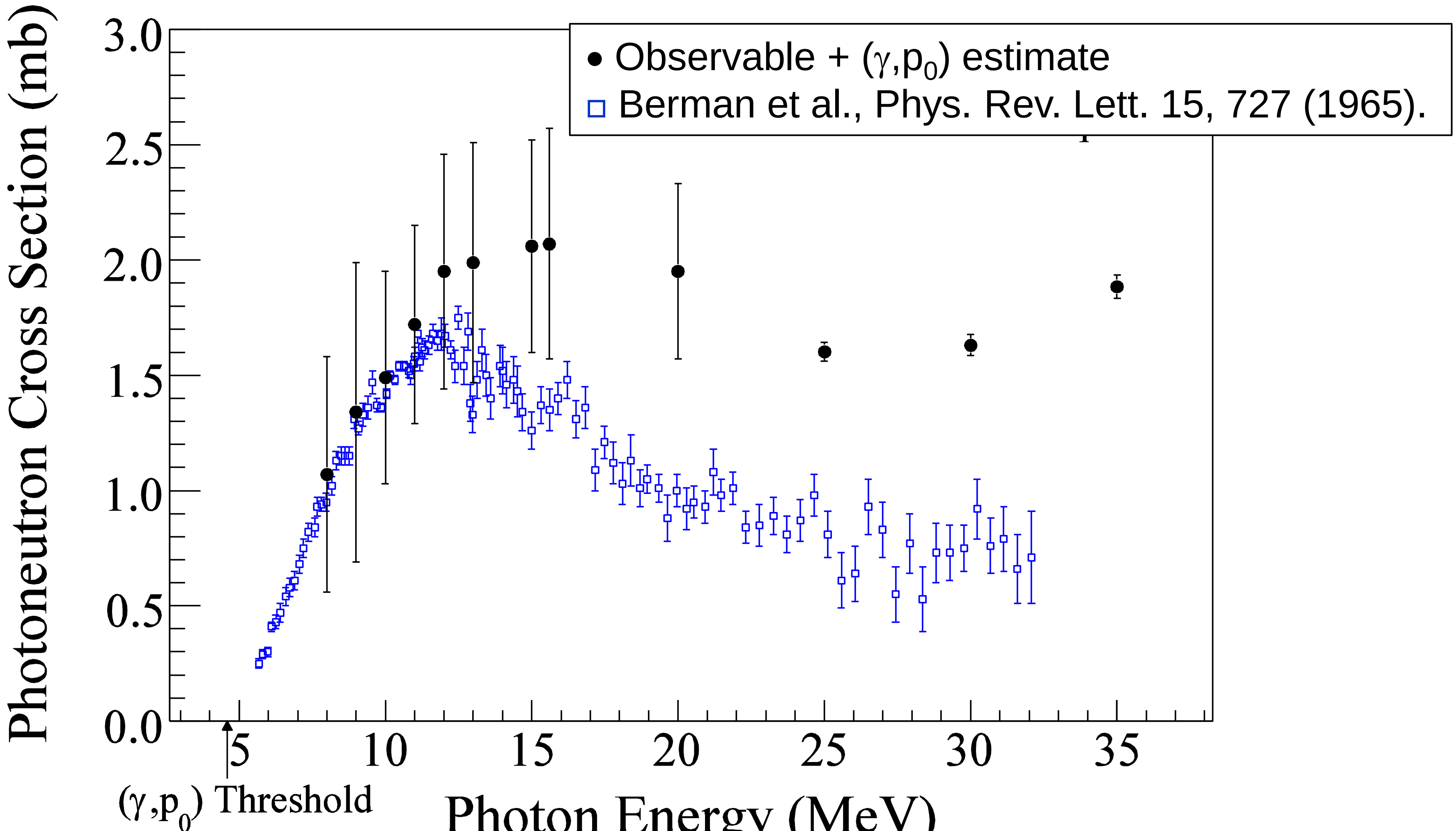

Comparison to Theory

- To compare to the theoretical prediction for the total photoabsorption cross section we need to add an estimate for the (γ,^{3}He,^{3}H) reaction channel.
- This is the most important reaction channel that does not produce neutrons.
  - Significant disagreement between measurements.
  - We make an estimate by averaging existing data.

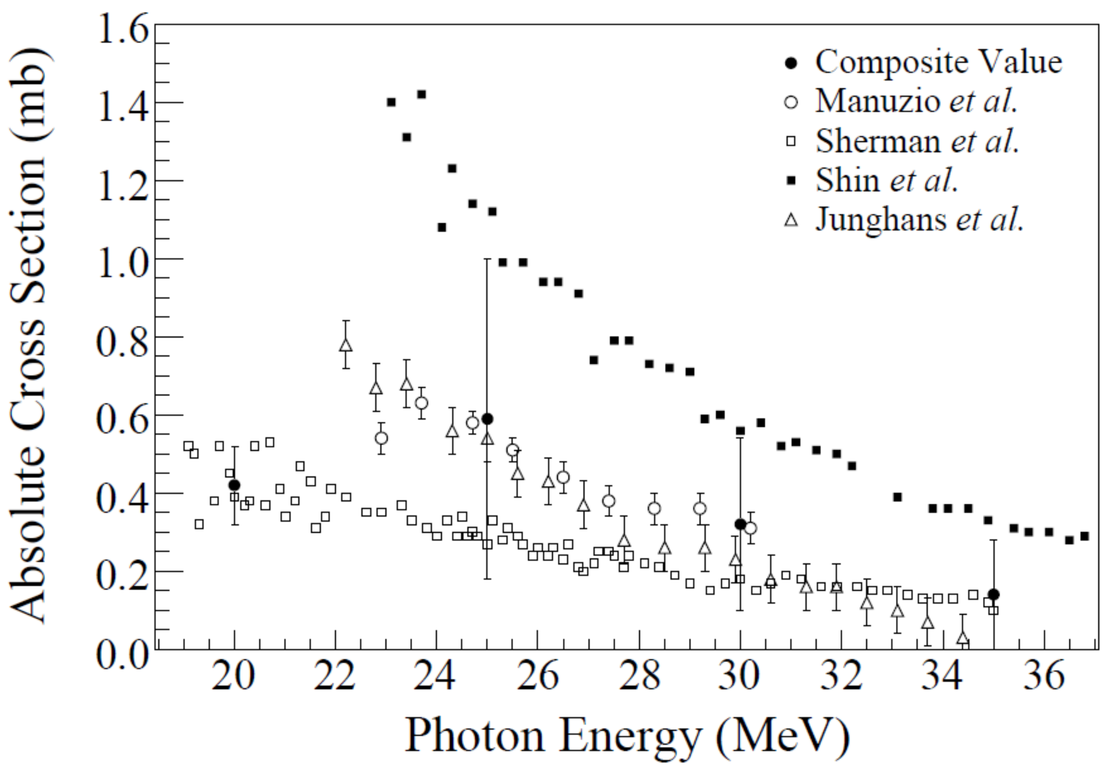

Comparison to Theory

- Large error bars are because of unmeasured reaction channels.

Bacca, *et al*., Phys. Rev. C **69**, 057001

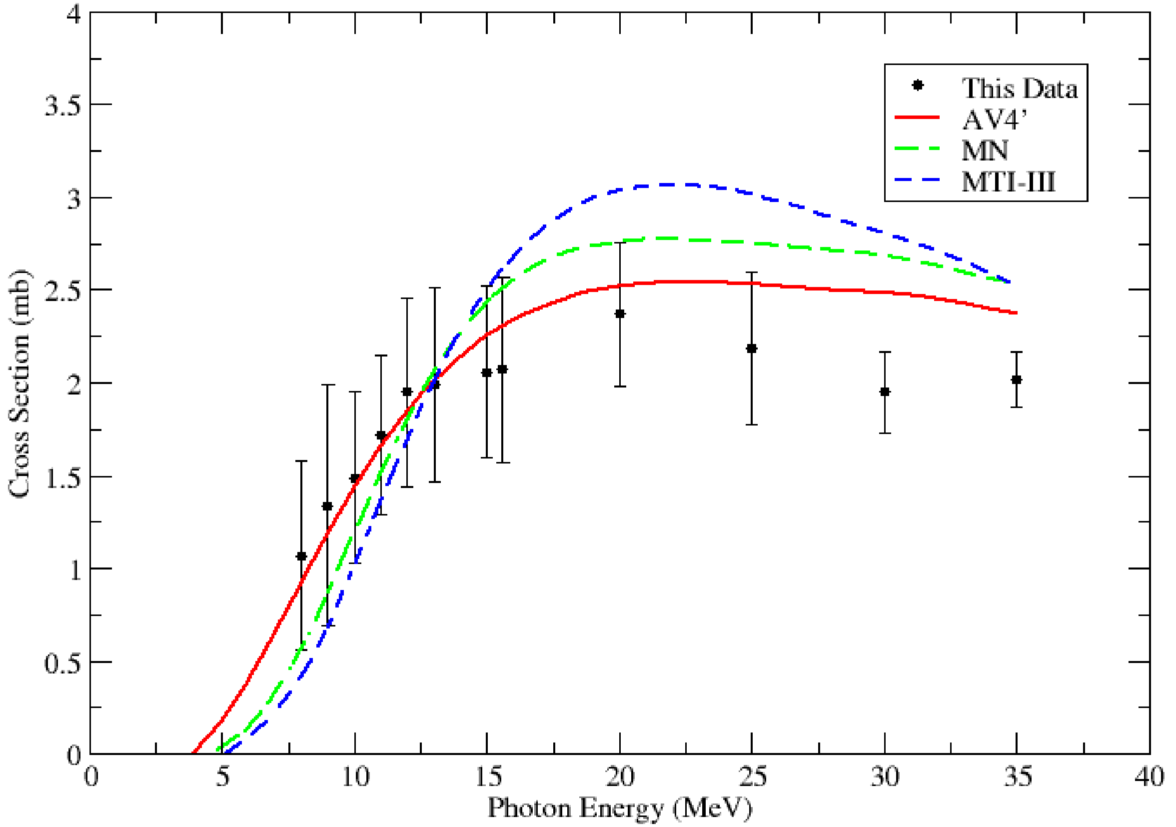

$^{7}Li(\gamma, n_0)$

- For ^{7}Li there are also many reaction channels.
- But for $^{7}Li(\gamma,n_0)$ a light output cut can be placed to eliminate other reaction channels.
- With such a high (1400 keV) light output cut there is perfect PSD separation.

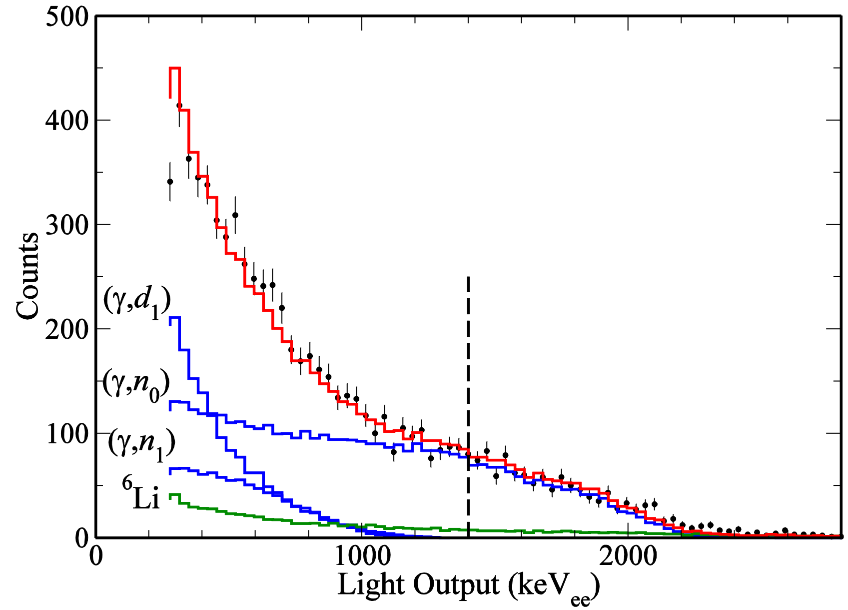

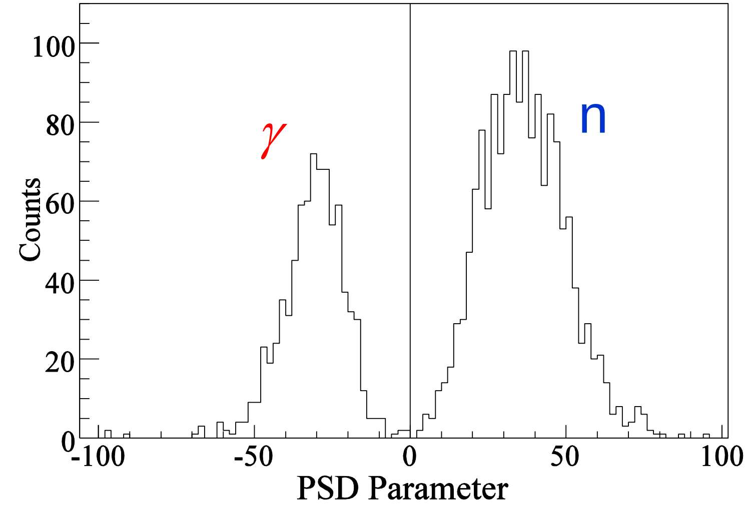

$^7Li(\gamma, n_0)$

- A fit can be done to the yield for each cell to extract the coefficients.
- Then the cross section can be calculated.

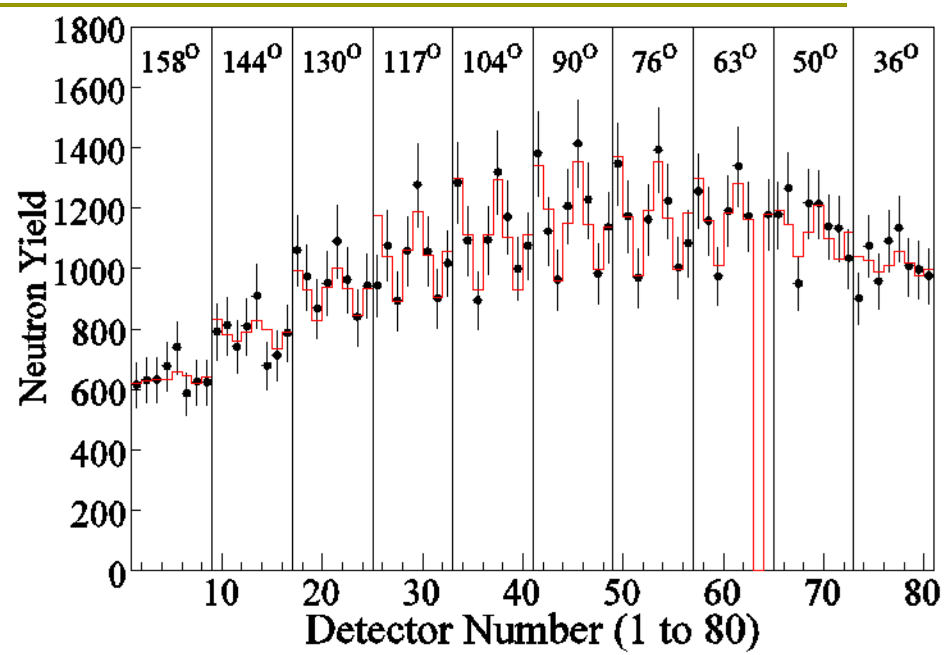

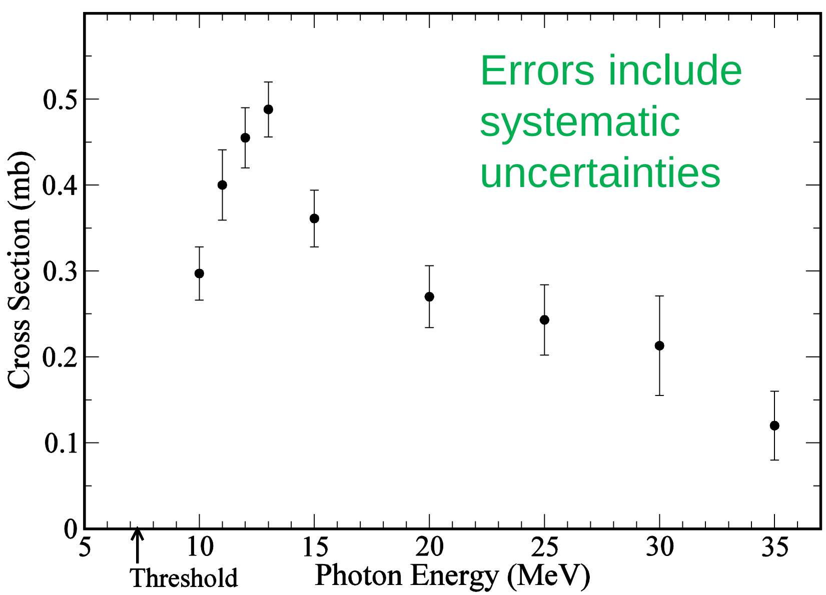

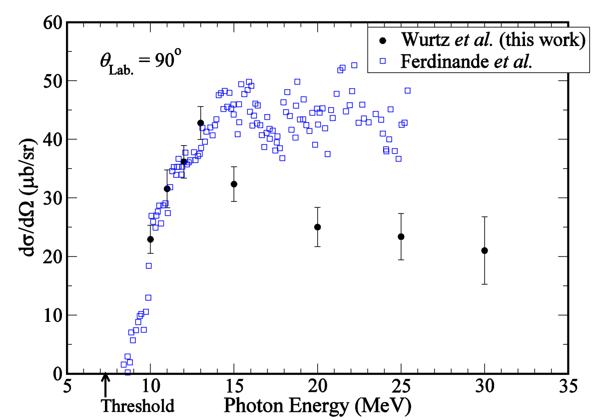

Wurtz et al. Phys. Rev. C 84 (2011) 044601

Summary

- Precision photoneutron measurements are now possible.
- Aiming for ~ 3% systematic uncertainties.
- Some data on Deuterium
- Some data on ^{6}Li and ^{7}Li
- GDH experiment – Early 2013
- ^{4}He experiment – Later 2013